Molecular Pharmacology Fast Forward. Published on June 29, 2012 as doi:10.1124/mol.112.078220
This article has not been copyedited and formatted. The final version may differ from this version.

MOL #78220

Title Page

Title: RNA Aptamer-based Functional Ligands of the Neurotrophin Receptor, TrkB

Authors Yang Zhong Huang, Frank J. Hernandez, Bin Gu, Katie R. Stockdale, Kishore Nanapaneni, Todd E. Scheetz, Mark A. Behlke, Andrew S. Peek, Thomas Bair, Paloma H. Giangrande, James O. McNamara II

Department of Neurobiology, Duke University Medical Center, Duke University, Durham, NC, USA. (Y.Z.H.)

Department of Internal Medicine, Roy J. and Lucille A. Carver College of Medicine, University of Iowa, Iowa City, IA, USA. (F.J.H., K.R.S., P.H.G., J.O.M.)

Department of Pharmacology and Cancer Biology, Duke University Medical Center, Duke University, Durham, NC, USA. (B.G.)

Center for Bioinformatics and Computational Biology, Roy J. and Lucille A. Carver College of Medicine, University of Iowa, Iowa City, IA, USA. (K.N., T.E.S.)

Department of Biomedical Engineering, Roy J. and Lucille A. Carver College of Medicine, University of Iowa, Iowa City, IA, USA. (K.N., T.E.S.)

Department of Ophthalmology and Visual Sciences, Roy J. and Lucille A. Carver College of Medicine, University of Iowa, Iowa City, IA, USA. (T.E.S.)

Integrated DNA Technologies (IDT), Coralville, IA, USA. (M.A.B., A.S.P.)

DNA Facility, University of Iowa, Iowa City, IA, USA. (T.B.)

Molecular Pharmacology Fast Forward. Published on June 29, 2012 as DOI: 10.1124/mol.112.078220
This article has not been copyedited and formatted. The final version may differ from this version.

Running Title Page

Running Title: Functional RNA Ligands for TrkB

Corresponding author James O. McNamara II, Ph.D.

Department of Internal Medicine

University of Iowa

375 Newton Road, Room 5204 MERF

Iowa City, IA 52242

Phone: 319-335-8491

E-mail: james-mcnamara@uiowa.edu

Figures 9

Tables 1

Number of text pages 26

References 35

Words

Abstract	199
Introduction	526
Discussion	1584

Abbreviations: AD, Alzheimer's Disease; ANOVA, analysis of variance; BDNF, brain-derived neurotrophic factor; BSA, bovine serum albumin; CCD, charge-coupled device; CNS, central nervous system; DMEM, Dulbecco's modified eagle medium; DNA, deoxyribonucleic acid; DPBS, Dulbecco's phosphate-buffered saline; ECD, extracellular domain; ECL, enhanced chemiluminescence; EDTA, Ethylenediaminetetraacetic acid; EEG, electroencephalogram; FAM, fluorescein amidite; FITC, fluorescein isothiocyanate; HEK, human embryonic kidney cells; HD, Huntington's Disease; HEPES, N-(2-Hydroxyethyl)piperazine-N'-(2-ethanesulfonic acid); KA, kainic acid; kDa, kilodaltons; kg, kilograms; LDH, lactate dehydrogenase; µl, microliters; µM, micromolar; ng, nanograms; nM, nanomolar; nm, nanometer; nmol, nanomole; NT4, neurotrophin-4; ml, milliliters; PBS, phosphate-buffered saline; PCR, polymerase chain reaction; PLCγ, phospholipase C-gamma; RNA, ribonucleic acid; RT, reverse transcription; RTK, receptor tyrosine kinase; SDS-PAGE, sodium dodecyl sulfate polyacrylamide gel electrophoresis; SELEX, Systematic Evolution of Ligands by EXponential enrichment; SEM, standard error of the mean; shRNA, short hairpin RNA; tRNA, transfer RNA;

Molecular Pharmacology Fast Forward. Published on June 29, 2012 as DOI: 10.1124/mol.112.078220
This article has not been copyedited and formatted. The final version may differ from this version.

Abstract

Many cell-surface signaling receptors, such as the neurotrophin receptor, TrkB, have emerged as potential therapeutic targets for diverse diseases. Reduced activation of TrkB in particular is thought to contribute to neurodegenerative diseases. Unfortunately, development of therapeutic reagents that selectively activate particular cell-surface receptors like TrkB has proven challenging. Like many cell-surface signaling receptors, TrkB, is internalized upon activation; in this proof of concept study, we exploited this fact to isolate a pool of nuclease-stabilized RNA aptamers enriched for TrkB agonists. One of the selected aptamers, C4-3, was characterized with recombinant protein binding assays, cell-based signaling and functional assays, and *in vivo*, in a seizure model in mice. C4-3 binds the extracellular domain of TrkB with high affinity (K_D~2nM), exhibits potent TrkB partial agonistic activity and neuroprotective effects in cultured cortical neurons. In mice, C4-3 activates TrkB upon infusion into the hippocampus; systemic administration of C4-3 potentiates kainic acid induced seizure development. We conclude that C4-3 is a potentially useful therapeutic agent for neurodegenerative diseases in which reduced TrkB activation has been implicated. We anticipate that the cell-based aptamer selection approach used here will be broadly applicable to the identification of aptamer-based agonists for a variety of cell-surface signaling receptors.

Molecular Pharmacology Fast Forward. Published on June 29, 2012 as DOI: 10.1124/mol.112.078220
This article has not been copyedited and formatted. The final version may differ from this version.

Introduction

Signaling via the neurotrophin receptor, TrkB, is critical to diverse biological processes in the CNS, including neuronal survival and differentiation as well as synaptic structure, function, and plasticity. TrkB is widely expressed in the developing and mature mammalian central nervous system (CNS). The prototypic neurotrophin ligands of TrkB, brain-derived neurotrophic factor (BDNF) and neurotrophin-4 (NT4), are 14 kDa proteins that are packed and released from dense core vesicles of nerve terminals. The binding of BDNF to the TrkB extracellular domain (ECD) induces receptor dimerization and subsequent phosphorylation of tyrosine residues within the intracellular domain, thereby initiating downstream signaling, including MAPK and PLCγ pathways (Huang and Reichardt, 2001).

Dysregulation of TrkB signaling has been implicated in the pathogenesis of several CNS disorders, including neurodegenerative diseases. The expression of BDNF and activation of TrkB in cortical neurons is reduced in striatal neurons in Huntington's disease (Zuccato et al, 2001). Reduced BDNF protein levels were also found in the entorhinal cortex and hippocampus in humans with Alzheimer's disease (Zuccato and Cattaneo, 2009). Importantly, supplementing BDNF levels in the brain by viral expression reverses neural atrophy and ameliorates cognitive impairment in rodent and primate models of Alzheimer's disease (Nagahara et al, 2009). Thus enhancing activation of TrkB may limit neuronal degeneration and progression of some neurodegenerative diseases. However, excessive activation of TrkB is also sufficient to induce both epilepsy and neuropathic pain (Croll et al., 1999; Lahteinen et al, 2003; Coull et al, 2005; Hu and Russek, 2008; He et al, 2010). Ligands used to enhance TrkB activation for therapeutic purposes therefore must not excessively activate this receptor.

Partial agonists are one type of receptor ligand that is particularly well-suited to address this problem. A partial agonist is a receptor ligand that elicits a sub-maximal

Molecular Pharmacology Fast Forward. Published on June 29, 2012 as DOI: 10.1124/mol.112.078220
This article has not been copyedited and formatted. The final version may differ from this version.

level of receptor activation in comparison to that elicited by a full agonist. Thus, the features of a partial agonist may tilt the balance of TrkB signaling to a level with a beneficial effect yet prevent excessive activation of TrkB. Indeed, several partial agonists of neuronal receptors are clinically effective drugs including buspirone (serotonin 5-HT_{1A} receptor anxiety) (Robinson et al, 1990) and varenicline ($\alpha_4\beta_2$ nicotinic cholinergic receptor for smoking cessation) (Jorenby et al, 2006). Partial agonists for TrkB have not been described.

RNA aptamers (synthetic, structural RNAs), which typically bind a target protein with high affinity and specificity, are emerging as a novel class of therapeutic reagents with a variety of uses including anticoagulation and targeted therapeutic delivery (Keefe et al., 2010). One of the most intriguing features of RNA aptamer technology is that the aptamer identification process known as SELEX (Systematic Evolution of Ligands by EXponential enrichment) provides a versatile ligand discovery platform that can be tailored to enrich for receptor ligands with diverse *functional* properties. Thus we hypothesized that we could identify RNA aptamers that serve as partial agonists of TrkB.

Here we describe a novel, functional cell-based SELEX approach for the identification of TrkB agonists in mammalian cells. We identified a TrkB ECD-binding RNA aptamer that exhibits partial agonistic activity in cultured neurons and upon infusion into the mouse hippocampus *in vivo,* yet was also capable of limiting BDNF-mediated activation of TrkB.

Molecular Pharmacology Fast Forward. Published on June 29, 2012 as DOI: 10.1124/mol.112.078220
This article has not been copyedited and formatted. The final version may differ from this version.

Materials and Methods

Reagents

BDNF was purchased from Chemicon. Other reagents were obtained from Sigma unless specified otherwise. Full-length TrkB mammalian expression plasmid pcDNA3-FLAG-TrkB was described previously (Huang and McNamara, 2010).

Cell culture and transfection

Cortical neuron/glia mixed cultures were prepared from embryonic 18 (E18) pups of pregnant Spraque-Dawley rat (Charles River) as described previously (Huang et al, 2008). The neurons were cultured in Neurobasal with B27 supplement and Glutamax (Invitrogen) for 12-24 days in vitro (DIV). HEK293 cells were maintained in DMEM medium supplemented with 10% fetal bovine serum. For plasmid DNA transfection, HEK293 cells were plated 12 h before transfection at a density of $5x10^5$ cells/well of 6-well culture plate and were transfected using Lipofectamine method (GIBCO BRL). 24 h after transfection, G418 (1mg/ml) was added to medium for 14 days. A single cell clone was selected and expanded. Animals were handled according to National Institutes of Health Guide for the Care and Use of the Laboratory Animals and approved by Duke University Animal Welfare Committee.

Cell Internalization SELEX

An RNA library consisting of 2'-fluoro pyrimidine modified RNAs, 51 nucleotides long with a central, 20 nucleotide variable region was prepared as described (McNamara et al, 2008). For library preparation, a template DNA oligo (5' TCGGGCGAGTCGTCTGNNNNNN NNN NNNNNNNNNNCCGCATCGTCCTCCC-3') and a 5'-oligo (5'-TAATACGACTCACT ATAGGGAGGACGATGCGG) (both synthesized by Integrated DNA Technologies (IDT), Coralville, IA) were annealed and extended with

Molecular Pharmacology Fast Forward. Published on June 29, 2012 as DOI: 10.1124/mol.112.078220
This article has not been copyedited and formatted. The final version may differ from this version.

Taq Polymerase (Denville Scientific, Inc.). The resulting duplex was used as template for *in vitro* transcription with a mutant (Y639F) T7 RNA Polymerase and the following nucleotide triphosphates: 1 mM ATP (Roche), 1 mM GTP (Roche), 3 mM 2'-fluoro-CTP (Trilink) and 3 mM 2'-fluoro-UTP (Trilink). Full-length RNA was gel-purified on a denaturing urea/acrylamide gel (RNA was visualized with UV-shadowing). 10% of the RNA recovered from cells after each cell-internalization procedure (outlined below) was reverse transcribed with a 3'-oligo (5'-TCGGGCGAGTCGTCTG-3') (IDT) using AMV Reverse Transcriptase (Roche); the RT reaction was then used as template in a 1 ml, 20-cycle PCR with 5'-oligo and 3'-oligo to generate the transcription template for the subsequent round of selection.

750 picomoles of library RNA were used for the first round; 500 picomoles of RNA were used in each subsequent round. The procedure for each round was as follows: A 150mm dish of HEK cells (~90% confluent) was first blocked by washing the cells twice with Dulbecco's Phosphate-Buffered Saline (DBPS) containing calcium and magnesium (Gibco) followed by incubation at 37ºC for 15 minutes in 15 milliliters DPBS supplemented with 100µg/ml yeast tRNA (Invitrogen).

To "pre-clear" the library, the DPBS/tRNA was replaced with 15 milliliters of DPBS containing the library and 100µg/ml yeast tRNA. After a 15 minute incubation at 37ºC, the supernatant was transferred to a centrifuge tube and spun at 2,500rpms in a table-top centrifuge in order to pellet cellular debris. Following centrifugation, the supernatant was transferred to a 150mm dish of TrkB-expressing HEK cells (~90% confluent) that had been blocked with tRNA as described for the HEK cells above. After a 20 minute incubation at 37ºC, with periodic gentle mixing, the supernatant was discarded. The cells were washed once with ice cold DPBS, once with ice cold 0.5 M NaCl and then incubated at 4ºC for 5 minutes in 20 milliliters of ice cold 0.5 M NaCl. After discarding the 0.5 M NaCl, cells were washed once with DPBS and then total RNA

Molecular Pharmacology Fast Forward. Published on June 29, 2012 as DOI: 10.1124/mol.112.078220
This article has not been copyedited and formatted. The final version may differ from this version.

was purified from the cells with Trizol (Invitrogen) extraction. Trizol extraction proceeded as outlined by manufacturer except that 2 µl of 5 mg/ml linear acrylamide (Ambion) was added to each aqueous phase (after chloroform addition) to facilitate RNA precipitation. The RNA pellet obtained from the Trizol procedure was suspended in 600 µl DPBS. The endogenous RNA was then digested at 37ºC for 25 minutes after addition of 6µl of RNAse A (Fermentas). RNA was then purified with phenol/chloroform/isoamyl alcohol and chloroform extractions, followed by ethanol precipitation. Each dried RNA pellet was dissolved in 50µl water and stored at -20ºC. A similar "pre-clearing" strategy was implemented for each subsequent round of selection.

454 Sequencing of the Round 4 PCR Product

The round 4 PCR product (1.1µM DNA duplex concentration) was diluted 1:100 with water and 1ul of this was used as template for a 20-cycle, 100ul PCR with the following primers (synthesized by IDT): Primer A.8 (5'-GCCTCCCTCGCGCCATC AG*G TCAGTCAAT*TAATACGACTCACTATAG) Primer B (5'-GCCTTGCCAGCCCGCTCAGT CGGGCGAGTCGTCTG). The 3' portions of each primer provided annealing (amplification) sites for the round 4 DNA duplex, while the 5' portions provided annealing sites for the 454 reaction. The italicized portion of Primer A.8 was used as a bar code, which allowed the inclusion of multiple, distinct PCR products in the 454 reaction. The PCR product was purified with a Qiagen Miniprep column and then combined with PCR products generated in the same manner (but with distinct bar codes) and submitted to the University of Minnesota sequencing facility. Sequences were clustered as previously described (Scheetz, et al., 2005).

Computational Comparison of Predicted Aptamer Secondary Structures

Molecular Pharmacology Fast Forward. Published on June 29, 2012 as DOI: 10.1124/mol.112.078220
This article has not been copyedited and formatted. The final version may differ from this version.

The most stable secondary structure of each unique aptamer sequence identified from the TrkB selection round 4 PCR product was predicted with the Vienna RNA Package Secondary Structure Prediction algorithm, version 2.0. This algorithm predicts RNA secondary structures based on an energy minimization algorithm. The structural similarities (tree distances) of the predicted structures were also computed with the Vienna Package and then output was written to a file that enabled graphical representation of the relationships with Cytoscape.

TrkB- SPR measurements

All measurements were performed with a Biacore 3000 at 37°C in DPBS running buffer (calcium chloride 0.901 mM, magnesium chloride 0.493 mM, potassium chloride 2.67 mM, potassium phosphate monobasic 1.47 mM, sodium chloride 137.93 mM and sodium phosphate dibasic 8.06 mM). Immobilization of ligands to CM5 and SA chips (GE Healthcare) followed standard procedures recommended by the manufacturer and protocols previously described (Hernandez, et al., 2009a, 2009b).

SELEX round SPR measurements

Recombinant mouse TrkB extracellular domain (R&D Systems) was immobilized on a CM5 sensor chip by amine coupling. Next, BDNF was injected at concentrations ranging from 10 to 100 nM to confirm the functionality of the immobilized TrkB protein. The assessment of the SELEX rounds was carried out by injecting 2.5 µM of each RNA pool at a flow rate of 15 µL/minute. Finally, the signals were aligned by BIA evaluation 4.1 software.

Determination of C4-3 Affinity for TrkB

Molecular Pharmacology Fast Forward. Published on June 29, 2012 as DOI: 10.1124/mol.112.078220
This article has not been copyedited and formatted. The final version may differ from this version.

The immobilization of C4-3 aptamer was performed by the streptavidin-biotin coupling method. C4-3 aptamer was previously biotinylated at 3'-end by periodate oxidation as previously described (Qin and Pyle 1999). The flow rate was set to 5 µL/minute, and the biotinylated C4-3 was injected at a concentration of 1 µM over the streptavidin surface (SA sensor chip) for 15 minutes at 25ºC. The unbound aptamer was removed by treatment with 50 mM aqueous NaOH and the chip was primed before use. TrkB protein solutions were sequentially injected over the sensor surface for 3 minutes at 15 µl/min and 3 minute dissociation time. Six concentrations of TrkB protein were injected by serially diluting samples from 400 to 12.5 nM. The selectivity studies were carried out by injecting 200 nM BSA and 200 nM TrkB protein over C4-3 aptamer and a control aptamer (4-1BB). The immobilization and injections for these control samples were performed under the same conditions described above. After each run, the surface was regenerated with 50 mM aqueous NaOH for 5 seconds at 15 µl/min. The raw data was processed and analyzed to determine the binding constant for C4-3 aptamer. To correct for refractive index changes and instrument noise, the response of the control surface data was subtracted from the responses obtained from the reaction surface using BIA evaluation 4.1. The K_D was calculated by global fitting of the six concentrations of TrkB protein assuming a constant density of C4-3 aptamer on surface. A 1:1 binding mode with mass transfer fitting was used to obtain the kinetic data. BSA and 4-1BB aptamer measurements were aligned to C4-3 aptamer and TrkB data for non-specific analysis.

Western blotting

Cultured neurons or HEK293 cells were lysed in modified RIPA buffer (10 mM Tris.HCl, pH 7.4, 1% Triton X-100, 0.1% sodium deoxycholate, 3 mM Na_3VO_4, 1mM EDTA, and protease inhibitors) and centrifuged at 16,000 g for 10 minutes; the

Molecular Pharmacology Fast Forward. Published on June 29, 2012 as DOI: 10.1124/mol.112.078220
This article has not been copyedited and formatted. The final version may differ from this version.

supernatant was defined as cell lysate. Mouse hippocampus was homogenized in a buffer containing 4 mM HEPES and 0.32M sucrose, pH 7.4. Cell lysates (10-20 µg) or homogenates were resolved by SDS-PAGE. The blots were incubated overnight with primary antibodies and subsequently with secondary antibodies (1:5000) for 1 hour at room temperature. The antibodies and dilution used in this study are as follows: p-Trk (pY515), p-Trk (pY705/706), p-Src (Y416), p-Akt, p-Erk (1:1000, Cell Signaling); TrkB (1:500, BD Transduction Laboratories); and β-actin (1:10,000, Sigma). p-TrkB (pY816) (1:1000) was kindly provided by Dr. Moses Chao (New York University). The immunoblots were developed with enhanced chemiluminescence (ECL, Amersham). Equivalent amount of protein loaded in each lane was verified with immunoblotting with antibodies to TrkB or actin. Immunoblots were scanned with a digital scanner and optical band density was quantified with ImageJ analysis software. Optical densities were normalized to actin levels. Data are presented as mean ± SEM. Results shown are representative of at least three independent immunoblotting experiments.

Fluorescence Microscopy: Localization of C4-3 on HEK cells

HEK cells and HEK cells expressing TrkB were grown on 35mm glass bottom MatTek culture dishes in DMEM supplemented with 10% FBS overnight. Cells were washed with pre-warmed DPBS and incubated for 1 hour at 37°C with FAM-labeled (FAM was on 3'-end) C4-3 or control aptamer (100µl of 100nM RNA) diluted in DPBS. Control aptamer (5'-GGGAGGACGAUGCGGUUUGGGGUUUUCCCGUGCCCCAGACGACUCGCCCGA-3') has identical modifications (2'-fluoro-modified pyrimidines) and fixed region sequences as C4-3, but a different variable region (underlined above). Next, cells were washed twice with ice cold DPBS followed by a 5 minute wash with 0.5M NaCl, 0.2N acetic acid at 4°C to remove unbound and surface-bound RNAs. Cells were then fixed with 4%

Molecular Pharmacology Fast Forward. Published on June 29, 2012 as DOI: 10.1124/mol.112.078220
This article has not been copyedited and formatted. The final version may differ from this version.

formaldehyde, 4% sucrose in DPBS for 20 minutes at room temperature. After fixation, the cells were permeabilized with 0.1% Triton X-100 in DPBS for 5 minutes and then incubated in block (5% goat serum plus 0.1% Triton X-100 in DPBS) for 1 hour at room temperature. The fluorescence signal of the FAM tag was enhanced by incubating with an anti-FITC antibody (rabbit anti-FITC ; 1:1000 dilution; Invitrogen catalogue# 71-1900) followed by a fluorescent secondary antibody (goat anti-rabbit IgG, Alexa Fluor 488-conjugate; 1:1000 dilution; Invitrogen catalogue# A11008). After labeling, cells were mounted with a glycerol mounting medium and a coverslip. Images of internalized aptamers were acquired with a 40x oil-immersion objective on an Olympus IX71 inverted microscope equipped with a cooled CCD camera and filters for FITC (excitation 450-490 nm, emission 515-565 nm). The fluorescence images shown are representative of at least three captured images per condition.

Cell death assay

Cell death was assessed by measuring lactate dehydrogenase (LDH) activity in culture supernatants by a spectrophotometric method (Whitney and McNamara, 2000). Data are presented as the means ± SEM of determinations made in six wells per condition from four independent experiments.

Hippocampal Interstitial Infusion

Animals were handled according to National Institute of Health Guide for the Care and Use of the Laboratory Animals and approved by Duke University Animal Care and Welfare Committee. Adult mice were anesthetized with isoflurane (5% induction, 1.5% maintenance) and mounted in a stereotaxic apparatus. The skull was exposed, and a hole was drilled over the hippocampus (-2.5 mm AP, 2.2 mm ML). A 30-gauge infusion cannula (Plastics One, Inc, Roanoke, VA) connected to a Hamilton syringe

Molecular Pharmacology Fast Forward. Published on June 29, 2012 as DOI: 10.1124/mol.112.078220
This article has not been copyedited and formatted. The final version may differ from this version.

(Hamilton Company, Reno, NV) via plastic tubing, was lowered into the hippocampus (1.8 mm DV), and vehicle, scrambled, or C4-3 aptamer was infused into the hippocampus at a flow rate of 0.1 µl/min over a period of 20 minutes using a calibrated syringe pump (Harvard Apparatus, Holliston, MA). Animals were sacrificed 30 minutes following start of infusion, brains were removed and hippocampus was isolated.

KA amygdala infusion

Continuous limbic and tonic-clonic seizures (status epilepticus) were induced in awake, adult male WT C57BL/6 mice (Mouri et al, 2008) weighing 20-25g by stereotaxic microinjection of 0.3µg kainic acid (KA, Sigma-Aldrich, St Louis, MO, USA) in a volume 0.5µL of PBS (pH 7.4) at 0.11µL/min into the right basolateral amygdala nucleus through a guide cannula (Plastics One, Inc., Roanoke, VA, USA). At least seven days prior to infusion of KA, the guide cannula was implanted in the right amygdala under pentobarbital anesthesia using the following stereotaxic coordinates relative to bregma: AP, -0.94 mm; ML, +2.85mm; and DV, -3.75mm; additionally, a bipolar EEG recording electrode was placed into the left dorsal hippocampus: -2.00 mm AP; -1.60mm ML; and -1.53mm DV. Either PBS or Scrambled (Scr) aptamer or C4-3 aptamer (200 nmol/kg) was injected intravenously through tail vein 15 minutes prior to KA infusion. EEG and behavior were monitored by an EEG recording device (Grass Technologies, Inc., West Warwick, RI, USA) and video camera (Victor Company of Japan, Ltd., Yokohama, Japan) respectively for 45 minutes following infusion. EEG status epilepticus was defined as continuous electrographic seizures (including post-ictal depression and /or polyspikes).

Scoring of behavioral seizures

Molecular Pharmacology Fast Forward. Published on June 29, 2012 as DOI: 10.1124/mol.112.078220
This article has not been copyedited and formatted. The final version may differ from this version.

Behavioral seizures were scored based on modified Racine scale (Racine, 1972). In detail, Class 0, Normal behavior; Class 1, Behavioral arrest and rigid posture (with or without extended tail); Class 2, Head bobbing; Class 3, Unilateral forelimb clonus and bilateral forelimb clonus without rearing; Class 4, Rearing and bilateral forelimb clonus; Class 5, Rearing and falling, loss of posture; Class 6, Running and jumping.

Statistical Analysis

Data are presented as means ± standard errors of the mean. In KA amygdala infusion experiments, the PBS and Scr-Aptamer groups were combined into a single control group because of the absence of significant difference between them (Student T-test or Mann-Whitney U Test, $p>0.05$). Statistical significance was assessed with the Mann-Whitney U Test or one way ANOVA post-hoc t-tests unless noted otherwise.

Molecular Pharmacology Fast Forward. Published on June 29, 2012 as DOI: 10.1124/mol.112.078220
This article has not been copyedited and formatted. The final version may differ from this version.

Results

Internalization-based screen for TrkB-specific aptamers

The mechanism of activation of TrkB has been well studied. The external signals that mediate activation of TrkB are neurotrophins including BDNF and NT4, 14 kDa proteins packed in dense-core vesicle of nerve terminals. BDNF binds to the ECD of TrkB and induces receptor dimerization, leading to autophosphorylation of tyrosines within the intracellular domain and subsequent initiation of downstream signaling pathways. Once activated, surface TrkB is internalized into intracellular compartments. To search for RNA aptamers that activate TrkB, we sought to isolate RNAs bound to and subsequently internalized with murine TrkB expressed in mammalian cells. The initial step was to establish a mammalian cell line stably expressing TrkB. Towards that end, HEK293 cells were transiently transfected with a plasmid expressing murine TrkB. A single colony of G418-resistant and TrkB-expressing HEK cells was then selected. The presence of TrkB on the HEK cell surface was verified with immunofluorescence (Fig 1B). Importantly, incubation of TrkB expressing HEK cells with BDNF (10 ng/ml for 15 minutes) resulted in TrkB activation as evidenced by increased phosphorylation of TrkB and Erk MAPK, a signaling protein downstream of TrkB (Fig 1C).

This TrkB-HEK cell line was subsequently used to select for RNA aptamers that bind TrkB. To reduce the presence of aptamers binding molecules expressed on surface of HEK cells other than TrkB, the RNA library was “pre-cleared” by incubation with HEK cells lacking TrkB (Fig 1A and methods). Following pre-clearing, the supernatant containing the RNA library was incubated with TrkB-expressing HEK cells and RNA internalized by these cells was recovered, amplified by PCR, and the procedure was repeated.

Identification of TrkB aptamers by high-throughput sequencing

Molecular Pharmacology Fast Forward. Published on June 29, 2012 as DOI: 10.1124/mol.112.078220
This article has not been copyedited and formatted. The final version may differ from this version.

A 51-nucleotide, 2'-fluoro pyrimidine-modified RNA library was used for the selection. After 4 rounds, the ability of the RNA pools to bind the ECD of recombinant murine TrkB was measured with surface plasmon resonance. The selected RNA pools exhibited progressive increases in binding to TrkB, with the round 4 pool exhibiting the greatest binding (Fig 1D), implying an enrichment of TrkB-binding RNAs. The sequences of the round 4 aptamer pool were determined with the high-throughput 454 platform; a total of 7,896 sequencing reads were obtained for this round.

Reads with identical variable regions were grouped into clusters. The number of reads per cluster ranged from 1 to 8, with most clusters consisting of a single read (Fig 2A). The secondary structures of the RNA sequences were also predicted and compared. A graphical representation of the predicted structural similarity of the RNA sequences is shown in Fig 2B. Each sequence was represented with a node and nodes with related predicted structures were connected with lines. This analysis revealed the presence of many minimally related structural species (i.e., the nodes at the bottom of the figure), as well as two large groups of sequences with related structures. Several sequences were chosen from the largest clusters for further study (Table 1).

Selected aptamers activate TrkB signaling in cortical neurons

To test whether the selected aptamers can activate TrkB, the tyrosine phosphorylation of TrkB was monitored in aptamer-treated primary cultures of embryonic rat cortical neurons. Selected aptamers were prepared by *in vitro* transcription and gel-purified. Cortical neurons were incubated with vehicle, BDNF (10 ng/ml), or selected aptamers (200 nM) for 15 min. Cell lysates were subjected to SDS-PAGE followed by immunoblotting with p-TrkB antibodies. BDNF induced an increase in phosphorylation of TrkB as well as downstream signaling molecules, Akt and Erk, providing a positive control for TrkB activation (Fig 3A). Interestingly, a subset of aptamers, including C4-2,

Molecular Pharmacology Fast Forward. Published on June 29, 2012 as DOI: 10.1124/mol.112.078220
This article has not been copyedited and formatted. The final version may differ from this version.

C4-3, C4-6, C4-7, C5-2, and C5-3 was able to enhance the phosphorylation of TrkB, Akt, and Erk, indicating that these aptamers are TrkB agonists (Fig 3A). In contrast, other aptamers, including C4-1, C4-4, C4-5, and C5-1 were inert in this assay (Fig 3A and data not shown), thus indicating that the agonistic effects observed were not due to non-specific effects of RNA application. These results demonstrate RNA aptamers can function as agonists for TrkB.

C4-3 binds to the extracellular domain of TrkB

The observation that a subset of the selected aptamers activates TrkB signaling in cultured neurons suggests that these aptamers bind directly to the ECD of TrkB. To test this possibility, we selected an aptamer with agonist properties, C4-3, for further study. Whereas the initial characterization of C4-3 utilized enzymatically synthesized RNA, subsequent characterization was carried out with chemically synthesized C4-3. Surface plasmon resonance was used to directly assess binding of C4-3 to the ECD of TrkB in a cell-free context. Application of BDNF to a sensor chip with immobilized, recombinant TrkB ECD resulted in concentration dependent increases in resonance units, thus demonstrating the expected functionality of the recombinant TrkB ECD preparation (Fig 4A). Application of the TrkB ECD to a sensor chip with immobilized C4-3 resulted in an increase of resonance units (Fig 4B); the binding of C4-3 to TrkB ECD was specific as C4-3 did not bind a control protein, bovine serum albumin (BSA) (Fig 4B). The fact that a control aptamer (M12-23, 4-1BB-specific aptamer) also synthesized with 2'-fluoro modified pyrimidines, failed to bind the TrkB ECD (Fig 4C) indicates that the TrkB ECD is not a promiscuous binder of such chemically modified RNA. The binding of C4-3 to the TrkB ECD was a concentration dependent and high affinity interaction, with an equilibrium dissociation constant (Kd) of 2.1 nM (Fig 4D). Taken

Molecular Pharmacology Fast Forward. Published on June 29, 2012 as DOI: 10.1124/mol.112.078220
This article has not been copyedited and formatted. The final version may differ from this version.

together, these results demonstrate that C4-3 binds to the TrkB ECD in a cell free system in vitro.

C4-3 is specifically internalized by TrkB-expressing HEK cells

The fact that C4-3 was identified with a cell-internalization selection suggests that C4-3 may be internalized upon binding to TrkB on the surface of cells. To explore this possibility, the localization of C4-3 was studied after incubation with TrkB-expressing or TrkB-negative HEK cells (Fig 5). For this experiment, cells incubated for 1 hour at 37ºC with a FAM-labeled version of C4-3 (or a control sequence), were treated with a stringent wash to remove surface-bound RNA. Antibody-based detection of the FAM (following fixation and cell permeabilization) greatly improved the detection sensitivity of the internalized RNAs (KRS, unpublished observations). The C4-3 internalized by the TrkB-expressing cells (Fig 5A) exhibited a punctate pattern, superimposed on a diffuse fluorescence pattern. Many of the puncta appeared to be adjacent to the plasma membrane, possibly indicating the presence of C4-3 in recycling endosomes. The diffuse fluorescence may be the result of a portion of the internalized C4-3 escaping from the endosomal compartment. The amount of C4-3 internalized by HEK cells that did not express TrkB was substantially less (Fig 5B), thus indicating that the internalization of C4-3 seen in the TrkB-expressing cells is dependent on TrkB expression. The increased uptake of C4-3 by the TrkB-expressing cells was a C4-3-specific phenomenon as a control RNA sequence exhibited substantially less internalization into the TrkB-expressing cells (Fig 5C). These observations are consistent with the conclusion that C4-3 binds the TrkB ECD on the cell surface and is subsequently internalized.

C4-3 activates TrkB signaling in cultured neurons

Molecular Pharmacology Fast Forward. Published on June 29, 2012 as DOI: 10.1124/mol.112.078220
This article has not been copyedited and formatted. The final version may differ from this version.

The observations that C4-3 binds directly to TrkB in a cell-free system as well as to native TrkB expressed on mammalian cells led us to further characterize the agonistic activity of this aptamer. Consistent with its binding affinity (K_D~2.1 nM), low nM (2-20 nM) concentrations of C4-3 activated TrkB signaling in cultured cortical neurons as evidenced by enhanced phosphorylation of TrkB and Akt, a downstream signaling protein (Fig 6A and Fig 7A); C4-3 is thus a potent TrkB agonist. The activation of TrkB was specific to the sequence of C4-3 because a control aptamer with a scrambled variable region failed to enhance phosphorylation of TrkB (Fig 6B), demonstrating the specificity of C4-3's agonistic effect. Activation of TrkB by C4-3 was time dependent (Fig 6C); its peak activity was evident at 15 minutes and, like BDNF, waned after 2 hours of incubation (Fig 6C).

If C4-3 binds and activates TrkB *per se* in cortical neurons, knockdown of TrkB protein would be expected to reduce the agonistic activity of C4-3. We tested this idea with TrkB-shRNA-expressing lentiviral vectors (Huang et al, 2008). The expression of TrkB protein was largely reduced in TrkB-shRNA treated neurons (Huang et al, 2008 and Fig 6D). Consistent with our prediction, knockdown of TrkB protein in cortical neurons resulted in reduced pTrkB in both BDNF and C4-3-treated cortical neurons (Fig 6D), thus further demonstrating that C4-3 specifically activates TrkB signaling in cultured neurons. In this experiment, we found the basal pTrk level to be slightly increased in cells treated with the TrkB-shRNA lentivirus versus that of the control. This increase is possibly the result of the antibody cross-reacting with pTrkC, which may have been upregulated in response to the depletion of TrkB protein.

C4-3 partially inhibits BDNF-mediated activation of TrkB

Since both BDNF and C4-3 are able to bind and activate TrkB, we queried whether C4-3 and BDNF might have an additive or synergistic effect on TrkB signaling.

Molecular Pharmacology Fast Forward. Published on June 29, 2012 as DOI: 10.1124/mol.112.078220
This article has not been copyedited and formatted. The final version may differ from this version.

To address this question, cortical neurons were pre-incubated with varying concentrations of C4-3 or scrambled aptamer for 15 min followed by brief incubation of BDNF (2 ng/ml). Interestingly, the BDNF-mediated increase of p-TrkB was attenuated by C4-3 in a concentration-dependent manner (Fig 7A). The inhibition by C4-3 was dependent upon the concentration of BDNF in that 2ng/ml BDNF was inhibited more effectively than 5ng/ml BDNF (Fig 7A). This effect was specific to C4-3 as various concentrations of a scrambled aptamer did not inhibit BDNF-mediated activation of TrkB. (Fig 7B). Notably, persistence of enhanced TrkB phosphorylation was evident even with the highest aptamer concentration (200 nM) co-incubated with BDNF compared to vehicle (Fig 7A and 7B). Thus, in addition to C4-3's ability to activate TrkB signaling (Fig 6), C4-3 can partially inhibit BDNF-mediated activation of TrkB in a concentration-dependent manner.

C4-3 exerts neuroprotective effects on cultured cortical neurons

Because reduced expression of BDNF is thought to contribute to death of CNS neurons in animal models of HD and AD, we asked whether C4-3 exhibits neuroprotective effects on cultured cortical neurons. For this experiment, we acutely withdrew the B27 growth supplement from healthy cultures of cortical neurons, which results in cell death that can be rescued by BDNF. Cells were protected from *N*-methyl-D-aspartate receptor activation-dependent toxicity by addition of MK-801 (1 μM) to the culture. Following B27 withdrawal from the culture for 48 h, cell survival was assessed by measuring LDH release into the culture media (Lee and Chao, 2001). Neuronal cell death was induced upon B27 withdrawal (Fig 8A). Addition of BDNF (100 ng/ml) to the culture medium reduced cell death by about 40% (Fig 8A), confirming a previous report (Lee and Chao, 2001). Addition of C4-3 (2 nM) to the culture medium reduced cell death

Molecular Pharmacology Fast Forward. Published on June 29, 2012 as DOI: 10.1124/mol.112.078220
This article has not been copyedited and formatted. The final version may differ from this version.

by 30% whereas the scrambled aptamer was ineffective (Fig 8A), thereby demonstrating pro-survival effects of C4-3 on CNS neurons.

Effects of C4-3 *in vivo*

In order for a TrkB aptamer to have therapeutic utility, it must be able to activate TrkB *in vivo*. To determine whether C4-3 can activate TrkB *in vivo*, 2 µl of vehicle, C4-3 (2 µM) or scrambled aptamer (2 µM) was injected into the hippocampus of an adult mouse brain under isoflurane anesthesia. Thirty min after onset of infusion, the animals were sacrificed and hippocampal homogenates were prepared. Lysates were resolved with SDS-PAGE followed by immunoblotting. Infusion of C4-3 but not scrambled aptamer resulted in enhanced p-TrkB in hippocampus (Fig 9A), thereby demonstrating TrkB agonistic activity of C4-3 *in vivo*.

The biochemical evidence that C4-3 can activate TrkB *in vivo* led us to seek functional consequences of TrkB activation induced by C4-3 *in vivo*. This in turn led us to ask whether systemic treatment with C4-3 enhanced sensitivity to seizures evoked by the chemical convulsant, kainic acid (KA). That is, one consequence of enhanced TrkB activation *in vivo* is enhanced sensitivity to seizures evoked by kainic acid as evidenced by studies of mice with transgenic overexpression of either BDNF or TrkB (Croll et al, 1999; Lahteinen et al, 2003). To address this question, we employed a model in which seizures were induced by direct injection of KA into the right amygdala of a wild type mouse (Fig 9B and see details in Materials and Methods). Fifteen minutes prior to commencing infusion of KA, either C4-3 or a scrambled aptamer (200 nmol/kg) or vehicle alone was infused intravenously through the tail vein. Seizures were assessed by behavioral observation and electroencephalography, the latter detected with a bipolar recording electrode implanted in dorsal hippocampus contra-lateral to injection site. Following infusion of PBS or scrambled aptamer through the tail vein, the initial

Molecular Pharmacology Fast Forward. Published on June 29, 2012 as DOI: 10.1124/mol.112.078220
This article has not been copyedited and formatted. The final version may differ from this version.

electrographic seizure was detected 7.1 ± 0.9 min (n=7) following completion of KA infusion into the amygdala (Fig 9C left panel); continuous electrographic seizures (status epilepticus) ensued shortly thereafter (9.2 ± 0.95 min (n = 7) (Fig 9C right panel). In contrast to controls, infusion of C4-3 via tail vein 15 minutes prior to KA injection reduced both the latency to onset of the first EEG seizure (3.28 ± 1.02 min, n = 8) compared to control (7.1±0.9 min, n=7, p =0.0167, student's t-Test) and EEG status epilepticus (3.28 ± 1.02 min, n = 8) compared to control (9.2±0.95min, n=7, p=0.0009, student's t-Test). Likewise, compared to controls, infusion of C4-3 caused enhanced behavioral seizure responses to KA. The number of animals exhibiting seizures of behavioral class 4 or higher was increased in C4-3 pretreated mice (70 ±10%) as compared with that of control mice (33 ± 9%) (Fig 9E). Cumulative seizure scores during a period of 45min following KA infusion was increased in C4-3 pretreated mice compared to controls (Fig 9E). While a single control mouse (1/7) exhibited the most severe seizure (class 6), the majority of C4-3 pretreated mice (5/8) exhibited Class 6 seizures with shorter latency and longer duration (Fig 9D and E). Importantly, systemic infusion of C4-3 alone was not sufficient to induce seizures because infusion of C4-3 into tail vein followed by infusion of vehicle into the amygdala did not induce seizures (not shown). Moreover, directly infusing C4-3 (2 μM) into amygdala was not sufficient to induce seizures as detected by behavioral or electrophysiological measures (not shown). In summary, these results demonstrate that C4-3 enhances sensitivity to KA-induced seizures, a predicted functional consequence of enhanced activation of TrkB *in vivo*.

Molecular Pharmacology Fast Forward. Published on June 29, 2012 as DOI: 10.1124/mol.112.078220
This article has not been copyedited and formatted. The final version may differ from this version.

Discussion

The objective of this study was to identify an RNA partial agonist for TrkB. Towards that end, we developed a novel cell internalization SELEX approach based on the understanding that TrkB is internalized following binding of neurotrophins and subsequent receptor activation. In this proof-of-concept study, aptamers selected with this cell based functional screen were characterized with respect to their pharmacological, biochemical, and functional properties *in vitro* and *in vivo*. Several principal findings emerged. A subset of aptamers capable of activating TrkB signaling in cultured cortical neurons was identified. Characterization of one of these aptamers, C4-3, revealed that it bound the ectodomain of TrkB with high affinity (K_D ~2 nM) and potently and selectively activated TrkB signaling in cortical neurons. C4-3 also partially inhibited BDNF-mediated TrkB activation in cortical neurons, a property consistent with its classification as a partial agonist. C4-3 exerts neuroprotective effects in cortical neurons *in vitro.* Biochemical, electrophysiological, and behavioral measures indicate that C4-3 can activate TrkB in mouse brain *in vivo.* We conclude that C4-3 provides a potentially valuable therapeutic reagent for modulating activation of TrkB in diverse CNS disorders. Moreover this cell internalization SELEX approach may be broadly applicable for identifying aptamers with agonist, partial agonist, or antagonist properties for specific cell surface RTKs.

A cell-based functional screen for RTK RNA agonists

RTKs play a critical role in cell signaling by conveying extracellular stimuli to intracellular signaling pathways. Many members of the large RTK family have been implicated as key regulators of various cellular processes in health and disease. RTKs have thus emerged as promising therapeutic targets for a number of nervous system disorders (Lemmon and Schlessinger, 2010). Therapeutic approaches that target RTKs

Molecular Pharmacology Fast Forward. Published on June 29, 2012 as DOI: 10.1124/mol.112.078220
This article has not been copyedited and formatted. The final version may differ from this version.

for treatment of diverse diseases, including cancer and neurodegenerative diseases, have also been sought for many years.

A number of therapeutics targeting RTKs are in clinical use for treatment of cancer and other diseases (Lemmon and Schlessinger, 2010). These drugs are small molecules or monoclonal antibodies that bind the ectodomain of the RTK (Reichert and Valge-Archer, 2007). RNA aptamers represent an emerging class of therapeutics with some advantages over small molecule drugs and antibody-based therapeutics (Keefe et al., 2010). While small molecule drugs often suffer from difficult to explain off-target effects, RNA aptamers exhibit specificities and affinities comparable to those of antibodies. The aptamer identification process is considerably less complex and expensive than that for small molecules because screening for aptamers is carried out with a single complex mixture whereas each member of a (usually vast) small molecule library must be screened individually. In contrast to antibodies, aptamers can be produced economically with chemical synthesis, are amenable to chemical modification and have low immunogenicity. The ability to recover and identify a subset of RNAs from a complex library that exhibits desirable properties (in addition to target binding) in aptamer screens is another property that sets the aptamer platform apart.

The potential applications for RTK-selective aptamers have led others to search for aptamers specific for particular RTKs, including HER3, RET, and Tie2 (Chen, et al., 2003; Cerchia et al., 2005; White et al., 2008). Some of the aptamers that emerged from these selections exhibited antagonistic activity; however, aptamer agonists or partial agonists were not described. It is difficult to compare the outcomes of these selections with that for TrkB agonists described here. However, a plausible explanation for the absence of agonists from these screens is that incorporation of a functional component into aptamer screens may be necessary to sufficiently enrich for agonists.

Molecular Pharmacology Fast Forward. Published on June 29, 2012 as DOI: 10.1124/mol.112.078220
This article has not been copyedited and formatted. The final version may differ from this version.

For the TrkB aptamer selection, we sought to exploit the fact that RTK activation is usually followed by receptor/ligand co-internalization. By enriching for sequences that bound TrkB and were subsequently internalized, we expected to also enrich for sequences that activate the receptor. To identify the most prevalent sequences at a relatively early round of selection, we sequenced the selected pool with 454 sequencing technology, which yielded thousands of sequences. The functional activity of the selected aptamers was determined by measuring their impact on TrkB phosphorylation (pTrkB), a surrogate measure of TrkB activation. Interestingly, the majority of the 13 RNAs chosen for this characterization exhibited TrkB agonistic activity in cultured neurons (Fig 3A), thus demonstrating the efficiency of the functional aptamer selection.

C4-3 is a functional ligand for TrkB

"Partial agonist" refers to a molecule which binds to a receptor and stabilizes a conformation less productive for activation compared to a full agonist. Surface plasmon resonance experiments demonstrated that C4-3 bound to the ectodomain of TrkB with high affinity (Kd 2.1 nM) (Fig 4). C4-3 activated TrkB signaling in cortical neurons albeit less efficiently than the endogenous TrkB agonist, BDNF (Fig 6 A, C). Moreover, co-incubation of C4-3 with BDNF revealed a C4-3 concentration-dependent partial inhibition of BDNF-induced activation of TrkB (Fig 7 A, B). Collectively, these findings support the idea that C4-3 binds TrkB and stabilizes a less productive conformation compared to BDNF and should thus be classified as a partial agonist. Importantly, binding of TrkB by either BDNF or C4-3 would be expected to induce its internalization, an event that could limit activation of TrkB by extracellular ligands. If, as seems likely, the extent of internalization of TrkB induced by BDNF and C4-3 is similar, then receptor internalization induced by C4-3 is not sufficient to account for the antagonist activity of C4-3.

Molecular Pharmacology Fast Forward. Published on June 29, 2012 as DOI: 10.1124/mol.112.078220
This article has not been copyedited and formatted. The final version may differ from this version.

Importantly, the partial agonist activity of C4-3 proved sufficient to confer neuroprotective effects on cortical neurons *in vitro*. These effects were examined in cultures in which neuronal cell death was induced by B27 withdrawal from the culture medium. Addition of exogenous BDNF to these cultures prevented cell death (Fig 8A), demonstrating that enhancing TrkB activation promotes neuronal survival under these conditions. Likewise, C4-3, but not scrambled aptamer, potently reduced cell death in these cultures (Fig 8A), thereby demonstrating a neuroprotective effect of C4-3.

The evidence that C4-3 can selectively activate TrkB in cortical neurons and exert neuroprotective effects *in vitro* provided a strong rationale for determining whether C4-3 could activate TrkB *in vivo*. After direct infusion of C4-3 into mouse hippocampus *in vivo* the pTrk content was enhanced in hippocampal lysates in comparison to inactive controls (Fig 9A), thus demonstrating the agonist activity of C4-3 *in vivo*. To obtain physiological evidence of C4-3-mediated activation of TrkB *in vivo*, we examined the effects of C4-3 on the development of seizures induced by intra-amygdala infusion of KA. We chose this model because increased TrkB activation *in vivo* enhances sensitivity to seizures evoked by KA as shown by studies of mice that overexpress BDNF or TrkB (Croll et al, 1999; Lahteinen et al, 2003). Indeed, systemically administered C4-3 enhances the sensitivity and severity of KA evoked seizures. The mechanism by which C4-3 gains access to the brain in the context of this experiment is uncertain. Seizure activity locally in the kainate-infused amygdala may have resulted in transient breakdown of the blood-brain barrier and promoted access of C4-3 prior to emergence of behavioral seizures or EEG seizures detected in the contralateral hippocampus. Importantly, seizures were not elicited upon systemic administration of C4-3 when vehicle was infused into amygdala, nor with direct infusion of C4-3 into amygdala (not shown), thus demonstrating that C4-3 alone does not elicit seizures. Collectively, these

results suggest that C4-3 is a selective partial agonist of TrkB which confers neuroprotective effects *in vitro* and activates TrkB *in vivo*.

Advantages of TrkB partial agonists as therapeutic reagents

TrkB has emerged as a promising therapeutic target for a variety of diseases including neurodegenerative disorders. For instance, reduced expression of BDNF is thought to contribute to degeneration of striatal neurons in Huntington's disease (Zuccato et al, 2001). Moreover, BDNF levels are reduced in the entorhinal cortex and hippocampus of patients with Alzheimer's disease (Hock et al., 2000; Narisawa-Saito et al., 1996). Neuronal degeneration in these brain regions is a signature of Alzheimer's. Furthermore, increasing the levels of BDNF in the entorhinal cortex in rodent and primate models of Alzheimer's, has a neuroprotective effect and improves cognitive function (Nagahara et al., 2009). While these and other data provide a strong rationale for the pursuit of TrkB agonists as therapeutics for Alzheimer's, the present lack of optimal TrkB agonists for therapeutic applications presents an obstacle for such endeavors. Use of BDNF for therapeutic applications is limited by its side-effects (Ochs et al., 2000), which may result from the over-activation of TrkB (due to the additive concentrations of endogenous and exogenous BDNF) in non-diseased cells. Indeed, excessive activation of TrkB signaling in CNS neurons has deleterious consequences, including epilepsy and neuropathic pain (Croll et al., 1999; Lahteinen et al, 2003; Coull et al, 2005; Hu and Russek, 2008; He et al, 2010). Although several classes of artificial TrkB agonists have been developed, including peptide mimetics (O'Leary and Hughes, 2003), monoclonal antibodies (Qian et al, 2006), and diverse small molecules (Massa et al, 2010; Jang et al, 2010), these reagents appear to be full agonists and thus may suffer from the same drawbacks as BDNF.

Molecular Pharmacology Fast Forward. Published on June 29, 2012 as DOI: 10.1124/mol.112.078220
This article has not been copyedited and formatted. The final version may differ from this version.

These considerations led us to seek TrkB partial agonists, which would activate submaximal TrkB signaling while capping maximal activation levels (Tsai, 2007). The functional cell-based SELEX approach described herein permitted identification of C4-3, an aptamer that exhibits TrkB partial agonistic activity and neuroprotective effects *in vitro* and lacks unwanted seizure-inducing actions *in vivo*. Thus, C4-3 may prove to be a valuable reagent that can tilt the balance of TrkB signaling to a level with beneficial effects, yet prevent excessive activation of TrkB. Future studies will seek beneficial effects of C4-3 in mouse models of neurodegenerative disorders.

Molecular Pharmacology Fast Forward. Published on June 29, 2012 as DOI: 10.1124/mol.112.078220
This article has not been copyedited and formatted. The final version may differ from this version.

Acknowledgements

The authors wish to thank Dr. James O. McNamara, Sr. for many in depth discussions of this work and for critical feedback on the manuscript, Dr. William Thiel for critical feedback on the manuscript and Georgia Alexander for technical assistance with aptamer brain infusions.

Author Contributions

Participated in research design: Y. Z. H., F.J.H., P.H.G., J.O.M.

Conducted experiments: Y.Z.H., F.J.H., B.G., K.R.S., J.O.M.

Contributed new reagents or analytic tools: K.R.S., K.N., T.E.S., M.A.B., A.S.P., T.B., P.H.G., J.O.M.

Performed data analysis: Y.Z.H., F.J.H., B.G., K.R.S., K.N., T.E.S., T.B., J.O.M.

Wrote or contributed to the writing of the manuscript: Y.Z.H., J.O.M.

References

Cerchia, L., Duconge, F., Pestourie, C., Boulay, J., Aissouni, Y., Gombert, K., Tavitian, B., de Franciscis, V., and Libri, D. (2005). Neutralizing aptamers from whole-cell SELEX inhibit the RET receptor tyrosine kinase. PLoS Biol 3, e123.

Chen CH, Chernis GA, Hoang VQ, Landgraf R. (2003). Inhibition of heregulin signaling by an aptamer that preferentially binds to the oligomeric form of human epidermal growth factor receptor-3. Proc Natl Acad Sci U S A., 5;100(16):9226-31

Coull JA, Beggs S, Boudreau D, Boivin D, Tsuda M, Inoue K, Gravel C, Salter MW, De Koninck Y. (2005) BDNF from microglia causes the shift in neuronal anion gradient underlying neuropathic pain, Nature, 438(7070):1017-21.

Croll SD, Suri C, Compton DL, Simmons MV, Yancopoulos GD, Lindsay RM, Wiegand SJ, Rudge JS, Scharfman HE. (1999) Brain-derived neurotrophic factor transgenic mice exhibit passive avoidance deficits, increased seizure severity and in vitro hyperexcitability in the hippocampus and entorhinal cortex. Neuroscience, 93(4):1491-506.

He XP, Pan E, Sciarretta C, Minichiello L, McNamara JO. (2010). Disruption of TrkB-mediated phospholipase Cgamma signaling inhibits limbic epileptogenesis. J Neurosci. 30(18):6188-96.

Hernandez, F.J., Dondapati, S.K., Ozalp, V.C., Pinto, A., O'Sullivan, C.K., Klar, T.A., and Katakis, I. (2009a). Label free optical sensor for Avidin based on single gold nanoparticles functionalized with aptamers. J Biophotonics 2, 227-231.

Hernandez, F.J., Kalra, N., Wengel, J., and Vester, B. (2009b). Aptamers as a model for functional evaluation of LNA and 2 '-amino LNA. Bioorg Med Chem Lett 19, 6585-6587.

Hock, C., Heese, K., Hulette, C., Rosenberg, C., and Otten, U. (2000). Region-specific neurotrophin imbalances in Alzheimer disease: decreased levels of brain-derived neurotrophic factor and increased levels of nerve growth factor in hippocampus and cortical areas. Arch Neurol *57*, 846-851.

Hu Y, Russek SJ. (2008). BDNF and the diseased nervous system: a delicate balance between adaptive and pathological processes of gene regulation. J Neurochem. 105(1):1-17.

Huang, E.J., and Reichardt, L.F. (2001). Neurotrophins: roles in neuronal development and function. Annu Rev Neurosci 24, 677-736.

Huang YZ, Pan E, Xiong ZQ, McNamara JO.(2008). Zinc-mediated transactivation of TrkB potentiates the hippocampal mossy fiber-CA3 pyramid synapse. Neuron, 57(4):546-58.

Huang YZ, McNamara JO. (2010) Mutual regulation of Src family kinases and the neurotrophin receptor TrkB. J Biol Chem. 12;285(11):8207-17.

Jang SW, Liu X, Yepes M, Shepherd KR, Miller GW, Liu Y, Wilson WD, Xiao G, Blanchi B, Sun YE, Ye K. (2010). A selective TrkB agonist with potent neurotrophic activities by 7,8-dihydroxyflavone. Proc Natl Acad Sci U S A. 107(6):2687-92.

Jorenby DE, Hays JT, Rigotti NA, Azoulay S, Watsky EJ, Williams KE, Billing CB, Gong J, Reeves KR; **Varenicline** Phase 3 Study Group.(2006). Efficacy of varenicline, an

alpha4beta2 nicotinic acetylcholine receptor partial agonist, vs placebo or sustained-release bupropion for smoking cessation: a randomized controlled trial. JAMA. 2006 Jul 5;296(1):56-63.

Keefe AD, Pai S, Ellington A.(2010) Aptamers as therapeutics. Nat Rev Drug Discov. 2010 Jul;9(7):537-50.

Lahteinen, S., Pitkanen, A., Koponen, E., Saarelainen, T., and Castren, E. (2003). Exacerbated status epilepticus and acute cell loss, but no changes in epileptogenesis, in mice with increased brain-derived neurotrophic factor signaling. Neuroscience 122, 1081-1092.

Lee, F.S., and Chao, M.V. (2001). Activation of Trk neurotrophin receptors in the absence of neurotrophins. Proc Natl Acad Sci U S A 98, 3555-3560.

Lemmon, M.A., and Schlessinger, J. (2010). Cell signaling by receptor tyrosine kinases. Cell 141, 1117-1134.

Massa SM, Yang T, Xie Y, Shi J, Bilgen M, Joyce JN, Nehama D, Rajadas J, Longo FM. (2010). Small molecule BDNF mimetics activate TrkB signaling and prevent neuronal degeneration in rodents. J Clin Invest. 120(5):1774-85

McNamara, J.O., Kolonias, D., Pastor, F., Mittler, R.S., Chen, L., Giangrande, P.H., Sullenger, B., and Gilboa, E. (2008). Multivalent 4-1BB binding aptamers costimulate CD8+ T cells and inhibit tumor growth in mice. J Clin Invest 118, 376-386.

Mouri G, Jimenez-Mateos E, Engel T, Dunleavy M, Hatazaki S, Paucard A, Matsushima S, Taki W, Henshall DC. (2008). Unilateral hippocampal CA3-predominant damage and

short latency epileptogenesis after intra-amygdala microinjection of kainic acid in mice. Brain Res. 1213:140-51.

Nagahara, A.H., Merrill, D.A., Coppola, G., Tsukada, S., Schroeder, B.E., Shaked, G.M., Wang, L., Blesch, A., Kim, A., Conner, J.M., et al. (2009). Neuroprotective effects of brain-derived neurotrophic factor in rodent and primate models of Alzheimer's disease. Nat Med 15, 331-337.

Narisawa-Saito, M., Wakabayashi, K., Tsuji, S., Takahashi, H., and Nawa, H. (1996). Regional specificity of alterations in NGF, BDNF and NT-3 levels in Alzheimer's disease. Neuroreport *7*, 2925-2928.

Ochs, G., Penn, R.D., York, M., Giess, R., Beck, M., Tonn, J., Haigh, J., Malta, E., Traub, M., Sendtner, M., et al. (2000). A phase I/II trial of recombinant methionyl human brain derived neurotrophic factor administered by intrathecal infusion to patients with amyotrophic lateral sclerosis. Amyotroph Lateral Scler Other Motor Neuron Disord 1, 201-206.

O'Leary PD, Hughes RA. (2003). Design of potent peptide mimetics of brain-derived neurotrophic factor. J Biol Chem. 278(28):25738-44.

Qian MD, Zhang J, Tan XY, Wood A, Gill D, Cho S. (2006). Novel agonist monoclonal antibodies activate TrkB receptors and demonstrate potent neurotrophic activities. J Neurosci. 26(37):9394-403.

Qin, P.Z., and Pyle, A.M. (1999). Site-specific labeling of RNA with fluorophores and other structural probes. Methods 18, 60-70.

Racine, R.J. (1972) Modification of seizure activity by electrical stimulation. II. Motor seizure. Electroencephalogr Clin Neurophysiol 32(3):281-294

Reichert, J.M., and Valge-Archer, V.E. (2007). Development trends for monoclonal antibody cancer therapeutics. Nat Rev Drug Discov 6, 349-356.

Robinson DS, Rickels K, Feighner J, Fabre LF Jr, Gammans RE, Shrotriya RC, Alms DR, Andary JJ, Messina ME. (1990). Clinical effects of the 5-HT1A partial agonists in depression: a composite analysis of buspirone in the treatment of depression. J Clin Psychopharmacol,10(3 Suppl):67S-76S.

Scheetz, T.E., Trivedi, N., Pedretti, K.T., Braun, T.A., and Casavant, T.L. (2005). Gene transcript clustering: a comparison of parallel approaches. Future Gener Comp Sy 21, 731-735.

Tsai, S.J. (2007). TrkB partial agonists: potential treatment strategy for major depression. Med Hypotheses *68*, 674-676.

White RR, Roy JA, Viles KD, Sullenger BA, Kontos CD. (2008) A nuclease-resistant RNA aptamer specifically inhibits angiopoietin-1-mediated Tie2 activation and function. Angiogenesis. 2008;11(4):395-401

Whitney K.D. and McNamara J.O. (2000) GluR3 autoantibodies destroy neural cells in a complement-dependent manner modulated by complement regulatory proteins. J Neurosci, 1;20(19):7307-16.

Zuccato, C., Ciammola, A., Rigamonti, D., Leavitt, B.R., Goffredo, D., Conti, L., MacDonald, M.E., Friedlander, R.M., Silani, V., Hayden, M.R., et al. (2001). Loss of

huntingtin-mediated BDNF gene transcription in Huntington's disease. Science 293, 493-498.

Zuccato C, Cattaneo E. (2009). Brain-derived neurotrophic factor in neurodegenerative diseases. Nat Rev Neurol. 5(6):311-22.

Molecular Pharmacology Fast Forward. Published on June 29, 2012 as DOI: 10.1124/mol.112.078220
This article has not been copyedited and formatted. The final version may differ from this version.

Financial Support: FJH was supported by a postdoctoral fellowship from the American Heart Association. This work was supported by a grant from the National Institute of Neurological Disorders and Stroke [NS056217].

Footnotes

Duke University (B.G. & Y.Z.H.) and the University of Iowa (J.O.M., F.J.H. & P.H.G.) have applied for a patent on this technology. M.A.B. is employed by Integrated DNA Technologies, Inc., (IDT) which offers oligonucleotides for sale similar to some of the compounds described in the manuscript. IDT is however not a publicly traded company and this author does not personally own any shares/equity in IDT.

Molecular Pharmacology Fast Forward. Published on June 29, 2012 as DOI: 10.1124/mol.112.078220
This article has not been copyedited and formatted. The final version may differ from this version.

Legends for Figures

Fig 1. Cell-based internalization SELEX for selection of TrkB agonistic aptamers. (A) Schematic of selection. (B) Characterization of TrkB stably-transfected cells. HEK293 cells were transfected with either mock plasmid or TrkB-expressing plasmid pFLAG-TrkB. After incubation with G418 (1 mg/ml) for 14 days, a single cell clone was selected. Mock transfected or TrkB transfected cells were fixed with 4% paraformaldehyde followed by a 12 hr-incubation with TrkB antibody at 4ºC to label the portion of TrkB present on the cell surface; note that cells were not permeabilized when fixed. The anti-TrkB antibody was detected with a secondary antibody conjugated with Alexa Fluor 594 (red). Images shown are maximal projections of z-stack confocal images. (C) BDNF activates TrkB in TrkB stable cells. TrkB cells were incubated with vehicle or BDNF (10 ng/ml) for 15 min. Cell lysates were resolved with SDS-PAGE. The expression of TrkB protein was detected with immunoblotting with an antibody specific to TrkB. The activation of Trk was revealed by probing the blots with antibodies to p-Trk and p-Erk. (D) Surface plasmon resonance analysis of binding of SELEX rounds to immobilized recombinant TrkB ECD.

Fig 2. Identification of TrkB aptamers with high throughput sequencing. (A) Cluster analysis of 7,896 sequencing reads obtained via 454 high throughput sequencing of the round 4 RT-PCR product. While most sequences were read only one time, as indicated with the bar on the far left of the graph, several dozens of sequences were read 3 times or more. (B) TrkB cell selection, round 4 sequence clusters, grouped by similarity of predicted secondary structure. The subset of the total pool of unique sequences (2,805 of 6,761) that was found to have related secondary structures is illustrated. Sequence clusters that do not have predicted structures with tree distances (a measure of predicted secondary structure similarity) of 3 or fewer to others within the pool are not

Molecular Pharmacology Fast Forward. Published on June 29, 2012 as DOI: 10.1124/mol.112.078220
This article has not been copyedited and formatted. The final version may differ from this version.

illustrated. Each node represents an individual sequence cluster (i.e., a unique sequence). Blue lines indicate that the connected nodes have identical predicted secondary structures. Green, orange and red lines indicate structures separated by tree distances of 1, 2 or 3, respectively. Blue thus indicates greatest similarity and red indicates least similarity in predicted secondary structure. 445 families of sequences with related secondary structures were obtained. The largest and second-largest families are illustrated in the upper left and upper right corners, respectively, of the figure while the smallest families, consisting of pairs of nodes with related structures, are shown in the bottom of the figure.

Fig 3. Biochemical characterization of selected aptamers. Aptamers were synthesized by in vitro transcription and purified by acrylamide gel electrophoresis. Cortical neurons cultured from E18 rat pups were maintained in vitro for 12-14 days. Cortical neurons were incubated with vehicle, BDNF (10 ng/ml), or indicated aptamers (200 nM) for 15 min. Cell lysates were resolved onto SDS-PAGE. The blots were probed with indicated antibodies. The p-Trk antibody recognizes p-Trk pY816.

Fig 4. Surface Plasmon Resonance (SPR) measurements of binding of C4-3 to TrkB protein in a cell free system. (A) The functionality of a recombinant murine TrkB extracellular domain was evaluated by passing four different concentrations of recombinant BDNF over the surface immobilized protein. (B) Interaction of recombinant murine TrkB extracellular domain (applied at 200nM concentration (red trace)) with immobilized C4-3. Bovine serum albumin (applied at 200nM concentration (blue trace)) serves as a specificity control. (C) Application of 200nM recombinant murine TrkB extracellular domain to immobilized C4-3 (red trace) or immobilized 4-1BB aptamer (green trace) which serves as a specificity control. (D) High-affinity interaction between

Molecular Pharmacology Fast Forward. Published on June 29, 2012 as DOI: 10.1124/mol.112.078220
This article has not been copyedited and formatted. The final version may differ from this version.

immobilized C4-3 aptamer and TrkB recombinant extracellular domain. Six different TrkB concentrations were analyzed (12.5 to 400 nM – Data shown with red traces). A significant K_D value of 2.1nM was determined using Langmuir fitting (shown with black lines) with mass transfer.

Fig 5. C4-3 is specifically internalized by TrkB-expressing HEK cells. TrkB-expressing or TrkB-negative HEK cells were incubated with 100nM FAM-labeled C4-3 or control RNA for 1 hour at 37ºC. Surface-bound RNA was stripped from the cells with a salt/acid wash and then cells were fixed with formaldehyde, permeabilized and labeled with anti-FAM and fluorescent secondary antibodies. (A) TrkB-expressing HEK cells incubated with C4-3. (B) HEK cells incubated with C4-3. (C) TrkB-expressing HEK cells incubated with control RNA. Note evidence of C4-3 immunoreactivity signal within TrkB-expressing HEK cells (punctate (e.g., see arrows) and diffuse fluorescence in A) and signal absence in cells lacking TrkB (B). Signal detected with control RNA in TrkB-expressing HEK cells (C) provides a measure of non-specific uptake of RNA molecules of the size of C4-3 in these cells.

Fig 6. C4-3 increases phosphorylation of Trk receptors in cultured neurons. C4-3 aptamers were chemically synthesized and purified by HPLC. Cortical neurons cultured from E18 rat pups were maintained in vitro for 12-14 days. Cell lysates were resolved with SDS-PAGE. (A) Low nanomolar concentration of C4-3 was able to activate Trk receptors. Cortical neurons were incubated with vehicle, BDNF (10 ng/ml), or C4-3 with different concentrations for 15 min. (B) C4-3, but not scrambled aptamer (variable region sequence of “Scr” is: 5’-GACUAGCGAUCUGUUACGCA-3’) increased phosphorylation of Trk receptor. Cortical neurons were incubated with vehicle, C4-3, or scrambled aptamer (2 nM) for 15 min. (C) C4-3 increased phosphorylation of Trk receptors in a time

Molecular Pharmacology Fast Forward. Published on June 29, 2012 as DOI: 10.1124/mol.112.078220
This article has not been copyedited and formatted. The final version may differ from this version.

dependent manner. Cortical neurons were incubated with vehicle, BDNF (1 ng/ml), or C4-3 (2 nM) for indicated periods of time. (D) C4-3 induces phosphorylation of TrkB in a TrkB-requiring manner. Cortical neurons (DIV 6) were transduced with lentiviral vectors expressing either control- or TrkB-shRNA and then maintained for additional 14 days. Cortical neurons were incubated with vehicle, BDNF (1 ng/ml), or C4-3 (2 nM) for 15 min. The p-Trk antibodies recognize p-Trk pY515 (in A, B, and C) or p-Trk pY816 (in D). Quantitative analyses of relative levels of p-Trk and p-Akt are shown in bar graphs (number of experiments quantified includes 7 in A; 4 in B; and 5 in C). Statistical analyses were performed by one-way analysis of variance with post hoc test. *, indicates $p < 0.05$.

Fig 7. C4-3 partially inhibits BDNF-induced phosphorylation of TrkB in cultured neurons. C4-3 or scrambled aptamer was chemically synthesized and purified by HPLC. Cortical neurons cultured from E18 rat pups were maintained in vitro for 12-14 days. Cell lysates were resolved with SDS-PAGE. (A) C4-3 inhibited the phosphorylation of TrkB in a BDNF- and C4-3- concentration dependent manner. Cortical neurons were pre-incubated with vehicle or varying concentrations of C4-3 for 15 min and incubated for an additional 15 min in the presence of either vehicle or BDNF (2 ng/ml or 5 ng/ml). (B) C4-3, but not scrambled aptamer, reduced the phosphorylation of TrkB induced by BDNF. Cortical neurons were pre-incubated with vehicle, varying concentrations of C4-3 or scrambled aptamer for 15 min and incubated for an additional 15 min in the presence of BDNF (2 ng/ml). The p-Trk blots were probed with p-Trk (pY515) (in A and B) antibody. Quantitative analyses of relative p-Trk levels are shown in bar graphs (n = 4). Statistical analyses were performed by one-way analysis of variance with post hoc test. *, indicates $p < 0.05$.

Molecular Pharmacology Fast Forward. Published on June 29, 2012 as DOI: 10.1124/mol.112.078220
This article has not been copyedited and formatted. The final version may differ from this version.

Fig 8. C4-3 but not scrambled aptamer reduces neuronal cell death of cortical neurons in culture. Cortical neurons cultured from E18 rat pups were maintained in vitro for 12-14 days. Neuronal cell death was induced in primary cultures of rat cortical neurons (div 10) by withdrawal of B27 for 72 h. Cortical neurons were treated with BDNF (100 ng/ml), C4-3 or scrambled aptamer (2 nM) every 24 h. LDH was measured at 72 h after treatments. The histogram is summarized from 4 independent experiments with 6 replicates for each treatment. The statistical analysis was performed with one way ANOVA. * indicates $p<0.05$.

Fig 9. C4-3 activates TrkB *in vivo*. (A) Infusion of C4-3 but not scrambled aptamer activates TrkB *in vivo*. Adult mice were anesthetized with isoflurane during infusion. Animals were awakened following completion of infusion. Mouse hippocampi were infused with 2 µl of vehicle, C4-3, or scrambled aptamer (2 uM in PBS, 0.1 µl/min) over a 20 min-period. 30 min after onset of infusion, hippocampi were dissected and tissue homogenates were prepared. Proteins were resolved with SDS-PAGE. The blots were probed with indicated antibodies. The p-Trk blots were probed with p-Trk (pY705/706) antibody. Quantitative analysis of relative p-Trk levels is shown in bar graph (n = 3). Statistical analyses were performed by one-way analysis of variance with post hoc test. *, indicates $p < 0.05$. (B) Schematic of experiment. Five to seven days after surgery either PBS or Scr-aptamer or C4-3 aptamer (aptamers dissolved in PBS, 200 nMole/kg) was injected intravenously through tail vein 15min prior to KA amygdala infusion. Both EEG and behavior were monitored for 45min following infusion. The PBS (n=3) and Scr-aptamer (n=4) groups were combined into a single control group (n=7) compared to C4-3 (n=8) because of the absence of significant difference between them

Molecular Pharmacology Fast Forward. Published on June 29, 2012 as DOI: 10.1124/mol.112.078220
This article has not been copyedited and formatted. The final version may differ from this version.

(Mann-Whitney U Test or Student's t-Test, $p>0.05$). (C) C4-3 reduced the latency to onset of first electrographic seizure compared to control (left, Student's T-test, $*P<0.05$); and the latency to onset of EEG status epilepticus, which is defined by continuous electrographic seizures including post-ictal depression and/or polyspikes (right, Student's T-test, $***P<0.001$). (D) Time course of seizure severity in each control or C4-3 pretreated animal (panels on left, one mouse per row). The maximum seizure score of each animal was measured every 3min over a 45min period. The time scale in each box was 3 min. Note that blue boxes representing class 0 seizure-normal behavior were commonly found in the control group, whereas red boxes representing class 6 seizure-jumping and running were frequently observed in the C4-3 pretreated mice (left). Time course of average seizure scores evaluated every 3min over a 45min period (right, Two-way ANOVA, statistical significance was found between control and C4-3 pretreated groups, $***P<0.001$). (E) C4-3 increased the occurrence of class 4, 5 or 6 seizures (left lower) and cumulative seizure scores (left upper) compared to controls over a 45min period (Student's T-test, $*P<0.05$). C4-3 decreased the latency to class 6 seizures (right). Open circles, control (n=7); closed circles, C4-3 (n=8). Mann-Whitney U Test, $**P<0.01$.

Molecular Pharmacology Fast Forward. Published on June 29, 2012 as DOI: 10.1124/mol.112.078220
This article has not been copyedited and formatted. The final version may differ from this version.

Table 1. Variable Region Sequences of Aptamers From Largest Sequence Clusters

Variable Region Sequence	Cluster Size	Name
UCCGAGACUCCACUCAUCGC	8	C8
CAUCACUCGGCACAUCGCGU	6	C6
CAUAAGACCGCUGCUUGCCC	5	C5-1
UUAAACCUUCAGUCUUUGUG	5	C5-2
CGUUACUCGACUCCCCGUAU	5	C5-3
CCGGAUCUAUCCCUACACAU	5	C5-4
UUCCAGAUCUACCGCGCCUG	4	C4-1
CAACAUCCAGACUGGGACGU	4	C4-2
UCGUAUUAUCCGCUGCACGC	4	C4-3
GACACCAGUCAGGUCUUGGU	4	C4-4
UACACCGUACGUAUUUUCGC	4	C4-5
UAAAUCGGGCUCUAACGUGU	4	C4-6
UCCUGAACAAACAUACGCCA	4	C4-7

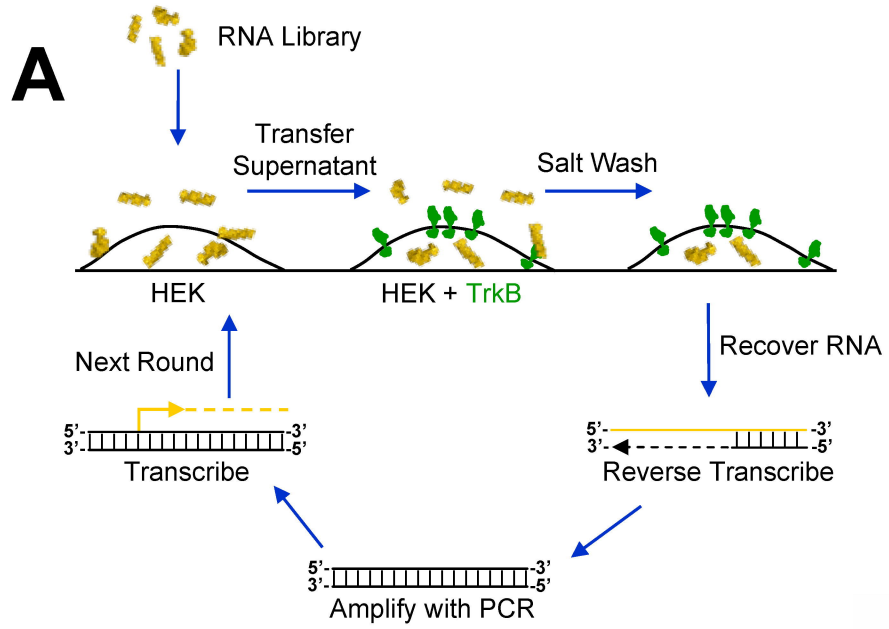
A
RNA Library
Transfer
Supernatant
Salt Wash
HEK
HEK + TrkB
Next Round
Recover RNA
5'
3'
3'
5'
Transcribe
Reverse Transcribe
Amplify with PCR

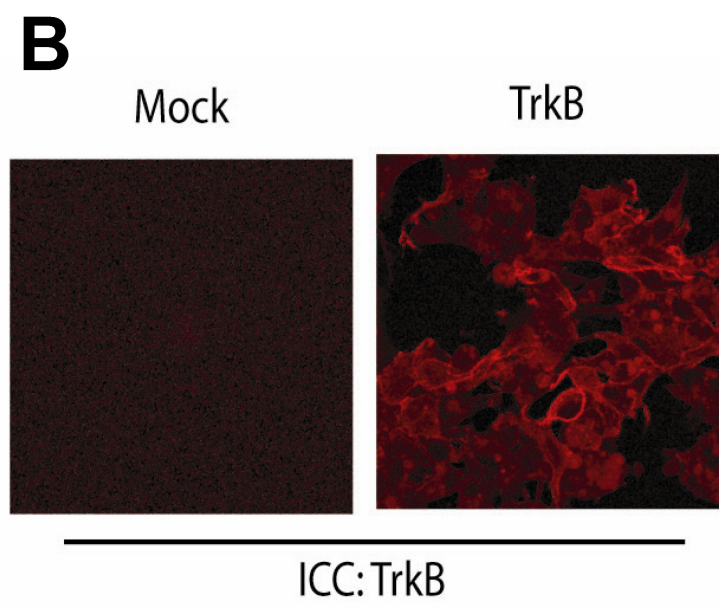
B
Mock
TrkB
ICC: TrkB

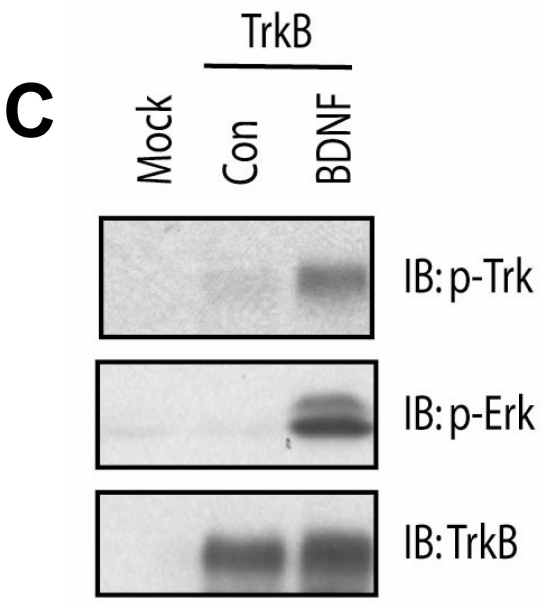
C
TrkB
Mock
Con
BDNF
IB: p-Trk
IB: p-Erk
IB: TrkB

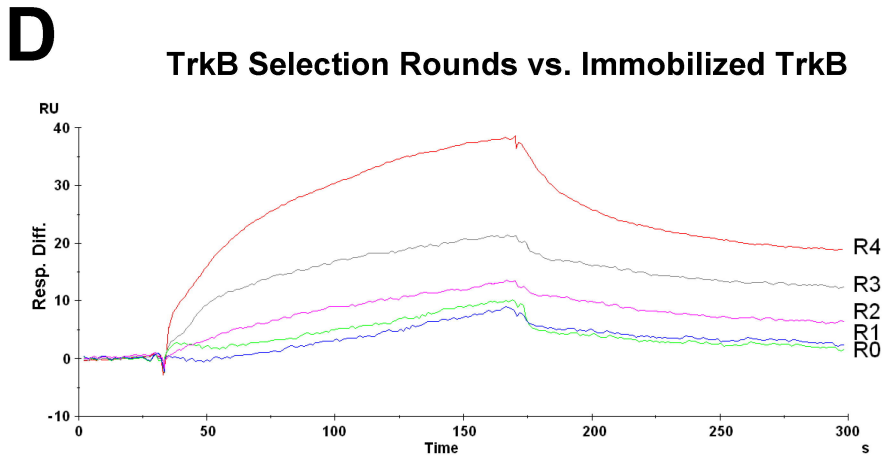
D
TrkB Selection Rounds vs. Immobilized TrkB
RU
Resp. Diff.
Time
s
R4
R3
R2
R1
R0

Fig 1

A

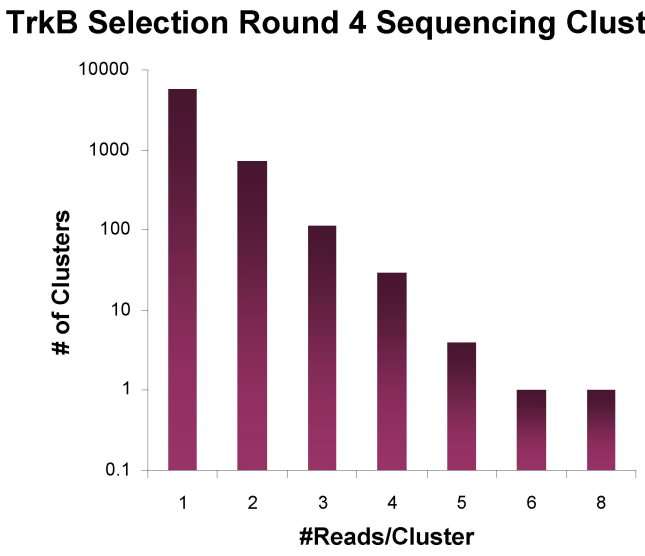
TrkB Selection Round 4 Sequencing Clusters
10000
1000
100
10
1
0.1
# of Clusters
1
2
3
4
5
6
8
#Reads/Cluster

B

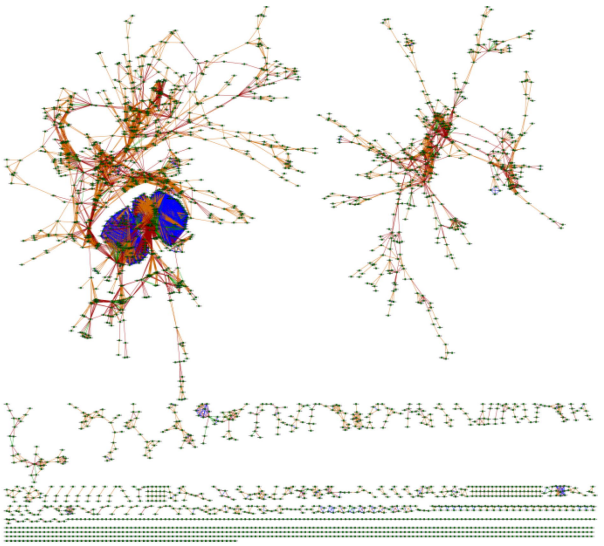

Fig 2

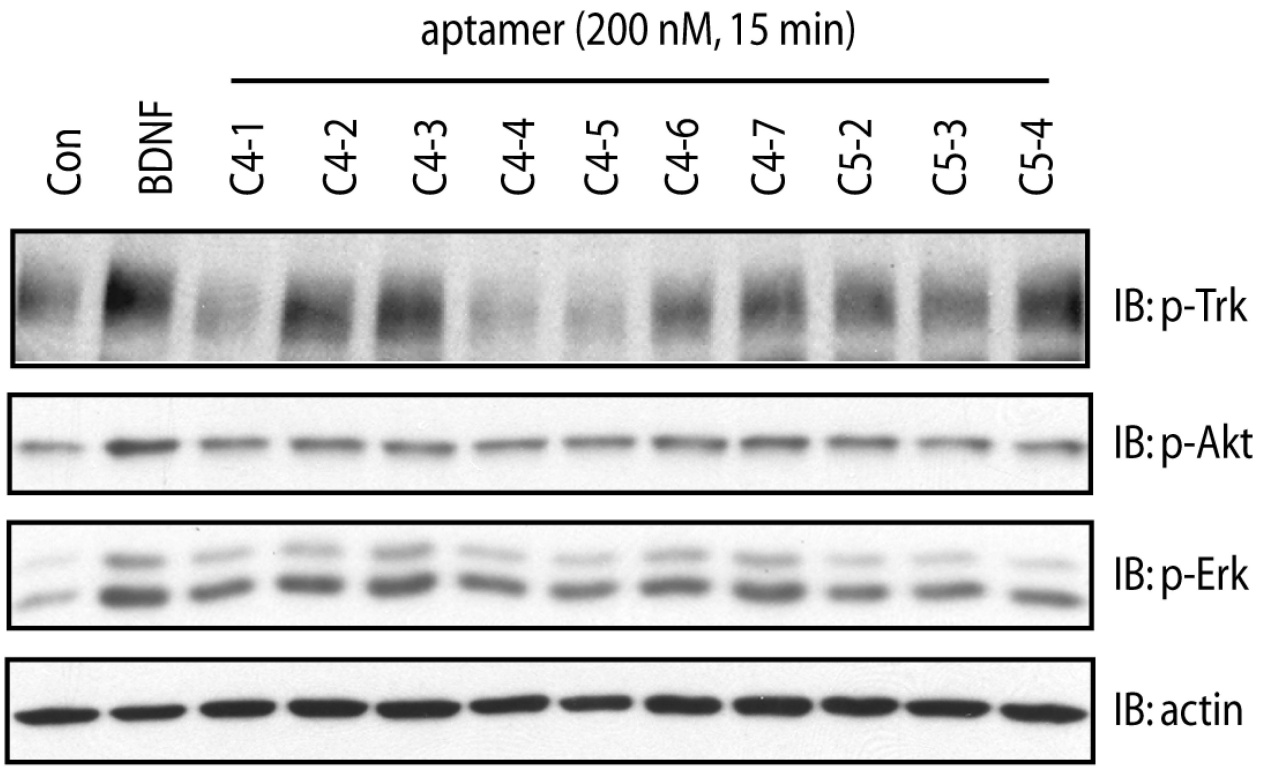
aptamer (200 nM, 15 min)
Con
BDNF
C4-1
C4-2
C4-3
C4-4
C4-5
C4-6
C4-7
C5-2
C5-3
C5-4
IB: p-Trk
IB: p-Akt
IB: p-Erk
IB: actin

Fig 3

Fig 4

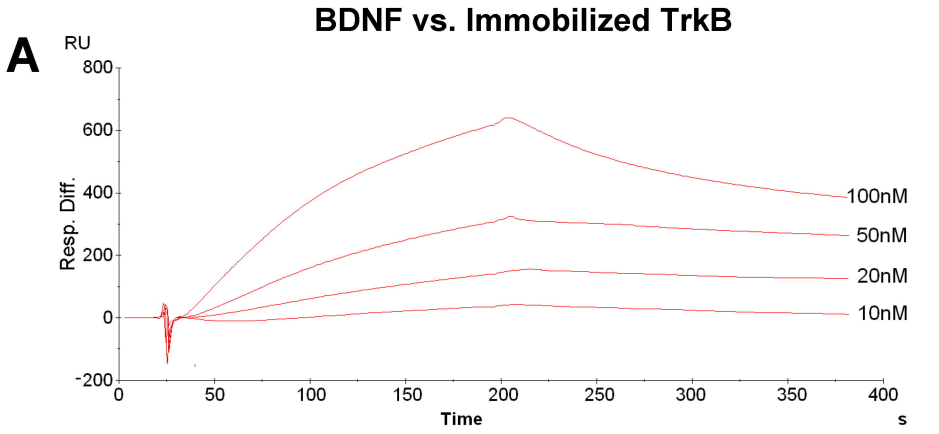
A
BDNF vs. Immobilized TrkB
RU
800
600
400
200
0
-200
Resp. Diff.
100nM
50nM
20nM
10nM
0
50
100
150
200
250
300
350
400
Time
s

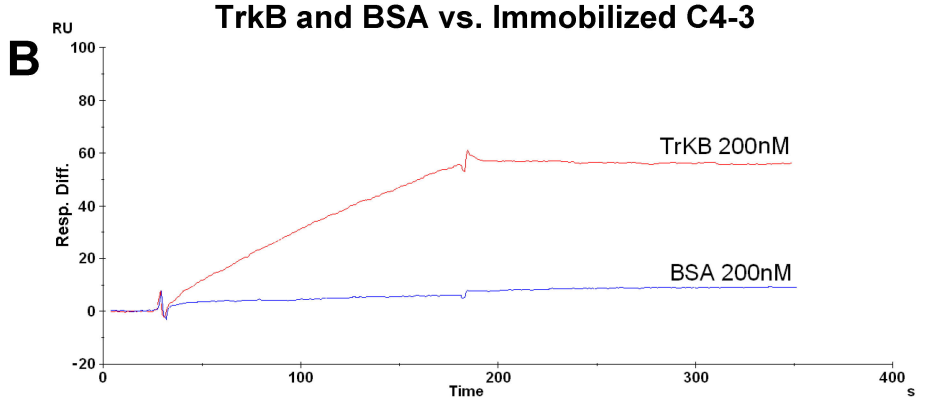
B
TrkB and BSA vs. Immobilized C4-3
RU
100
80
60
40
20
0
-20
Resp. Diff.
TrKB 200nM
BSA 200nM
0
100
200
300
400
Time
s

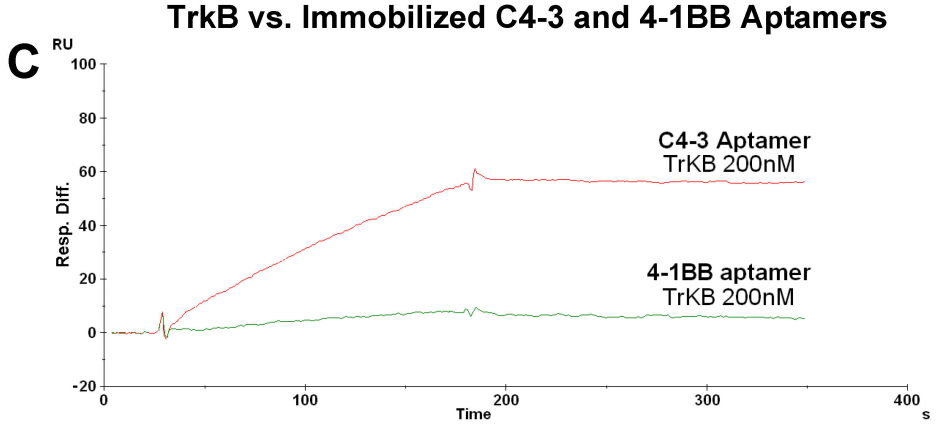
C
TrkB vs. Immobilized C4-3 and 4-1BB Aptamers
RU
100
80
60
40
20
0
-20
Resp. Diff.
C4-3 Aptamer
TrKB 200nM
4-1BB aptamer
TrKB 200nM
0
100
200
300
400
Time
s

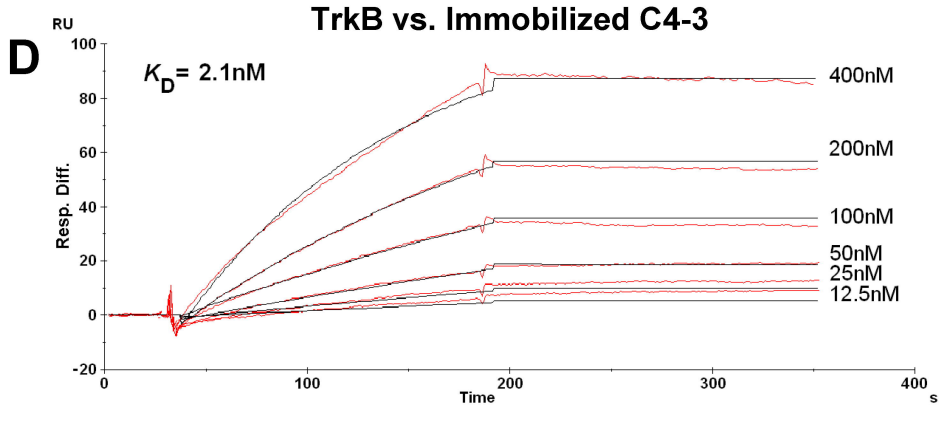
D
TrkB vs. Immobilized C4-3
RU
100
80
60
40
20
0
-20
Resp. Diff.
K_D= 2.1nM
400nM
200nM
100nM
50nM
25nM
12.5nM
0
100
200
300
400
Time
s

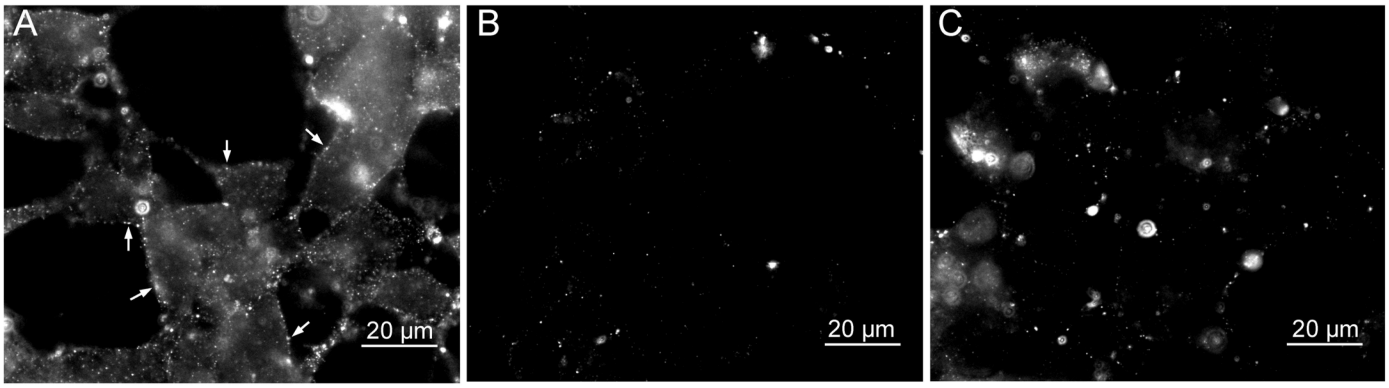

C4-3 + TrkB-HEK Cells | C4-3 + HEK Cells | Control RNA + TrkB-HEK Cells

Fig 5

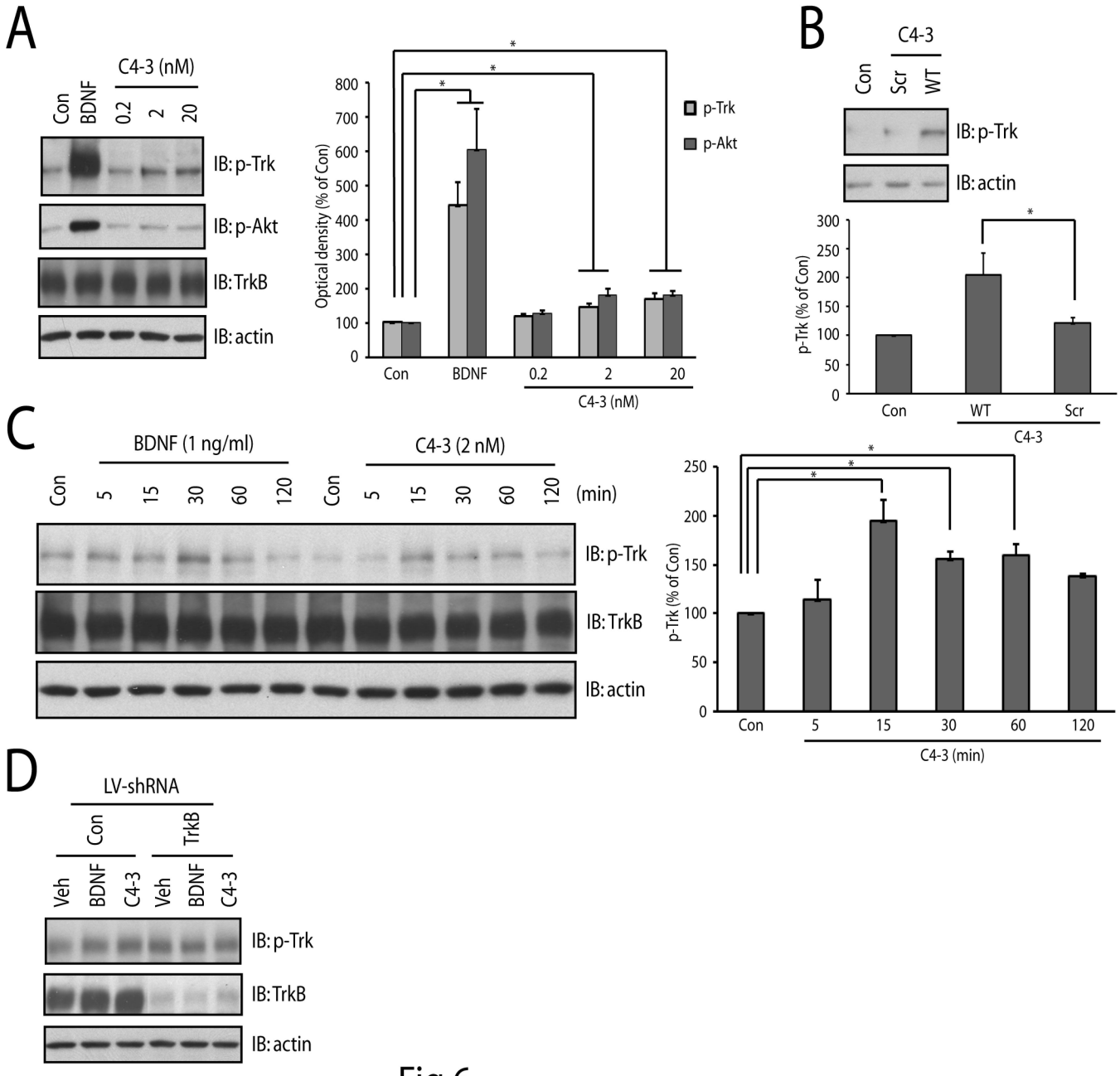
A
C4-3 (nM)
Con
BDNF
0.2
2
20
IB: p-Trk
IB: p-Akt
IB: TrkB
IB: actin
Optical density (% of Con)
p-Trk
p-Akt
Con
BDNF
0.2
2
20
C4-3 (nM)
B
C4-3
Con
Scr
WT
IB: p-Trk
IB: actin
p-Trk (% of Con)
Con
WT
Scr
C4-3
C
BDNF (1 ng/ml)
C4-3 (2 nM)
Con
5
15
30
60
120
(min)
IB: p-Trk
IB: TrkB
IB: actin
p-Trk (% of Con)
Con
5
15
30
60
120
C4-3 (min)
D
LV-shRNA
Con
TrkB
Veh
BDNF
C4-3
IB: p-Trk
IB: TrkB
IB: actin

Fig 6

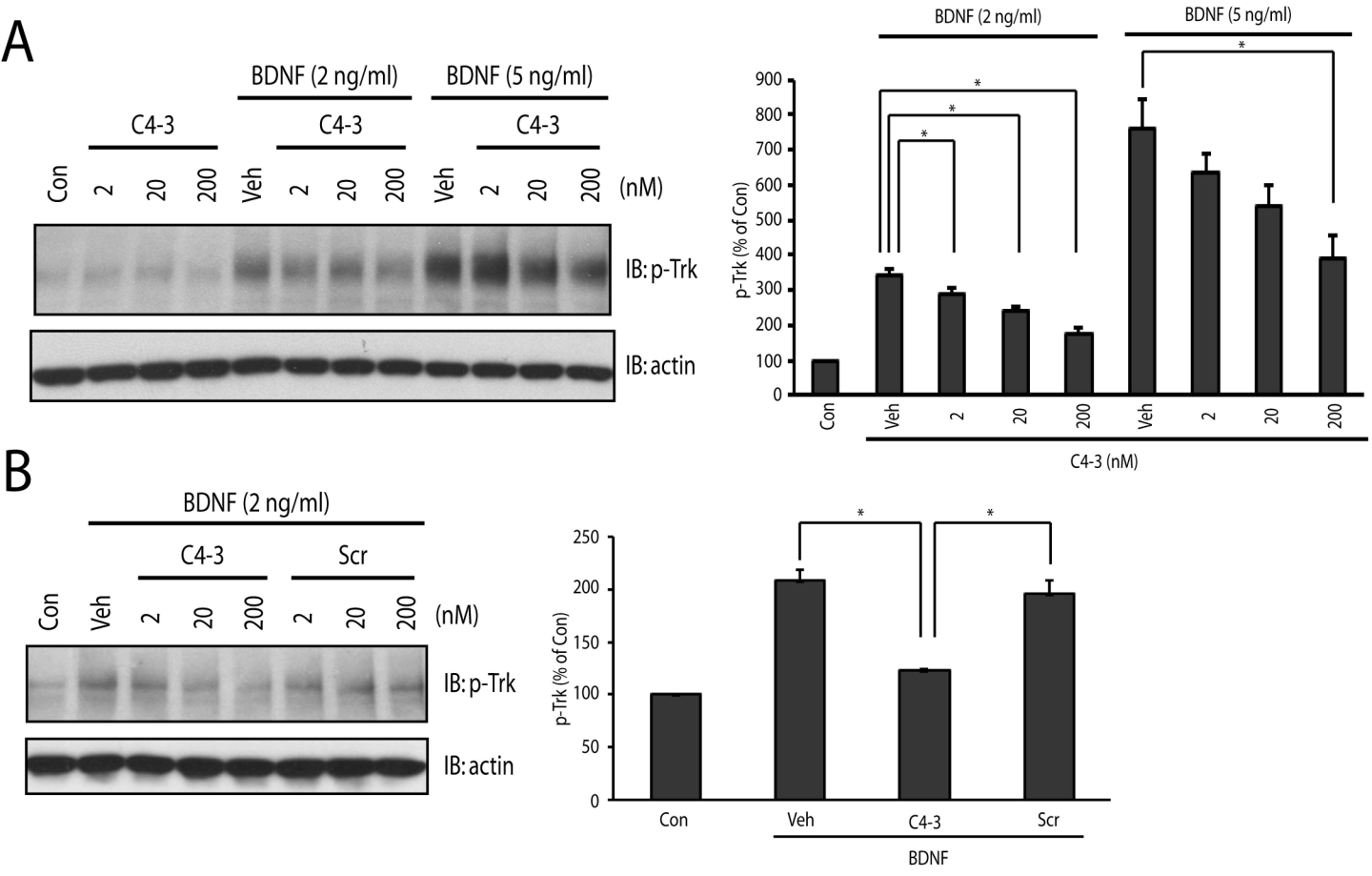
A
BDNF (2 ng/ml)
BDNF (5 ng/ml)
C4-3
C4-3
C4-3
Con
2
20
200
Veh
2
20
200
Veh
2
20
200
(nM)
IB: p-Trk
IB: actin
BDNF (2 ng/ml)
BDNF (5 ng/ml)
p-Trk (% of Con)
900
800
700
600
500
400
300
200
100
0
Con
Veh
2
20
200
Veh
2
20
200
C4-3 (nM)
B
BDNF (2 ng/ml)
C4-3
Scr
Con
Veh
2
20
200
2
20
200
(nM)
IB: p-Trk
IB: actin
p-Trk (% of Con)
250
200
150
100
50
0
Con
Veh
C4-3
Scr
BDNF

Fig 7

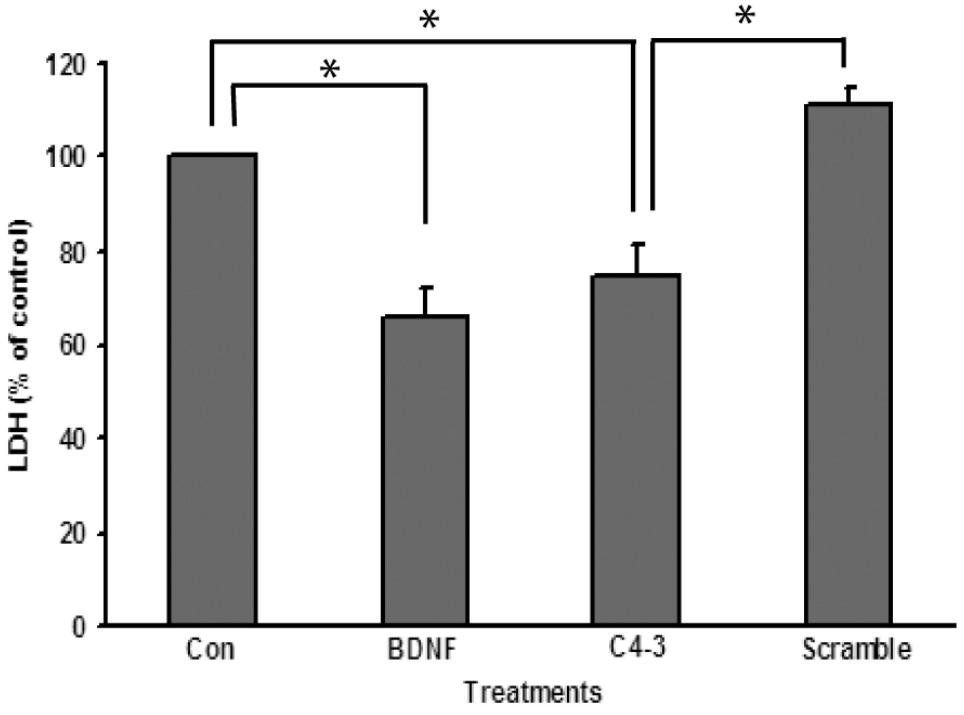
*
*
*
120
100
80
60
40
20
0
LDH (% of control)
Con
BDNF
C4-3
Scramble
Treatments

Fig 8

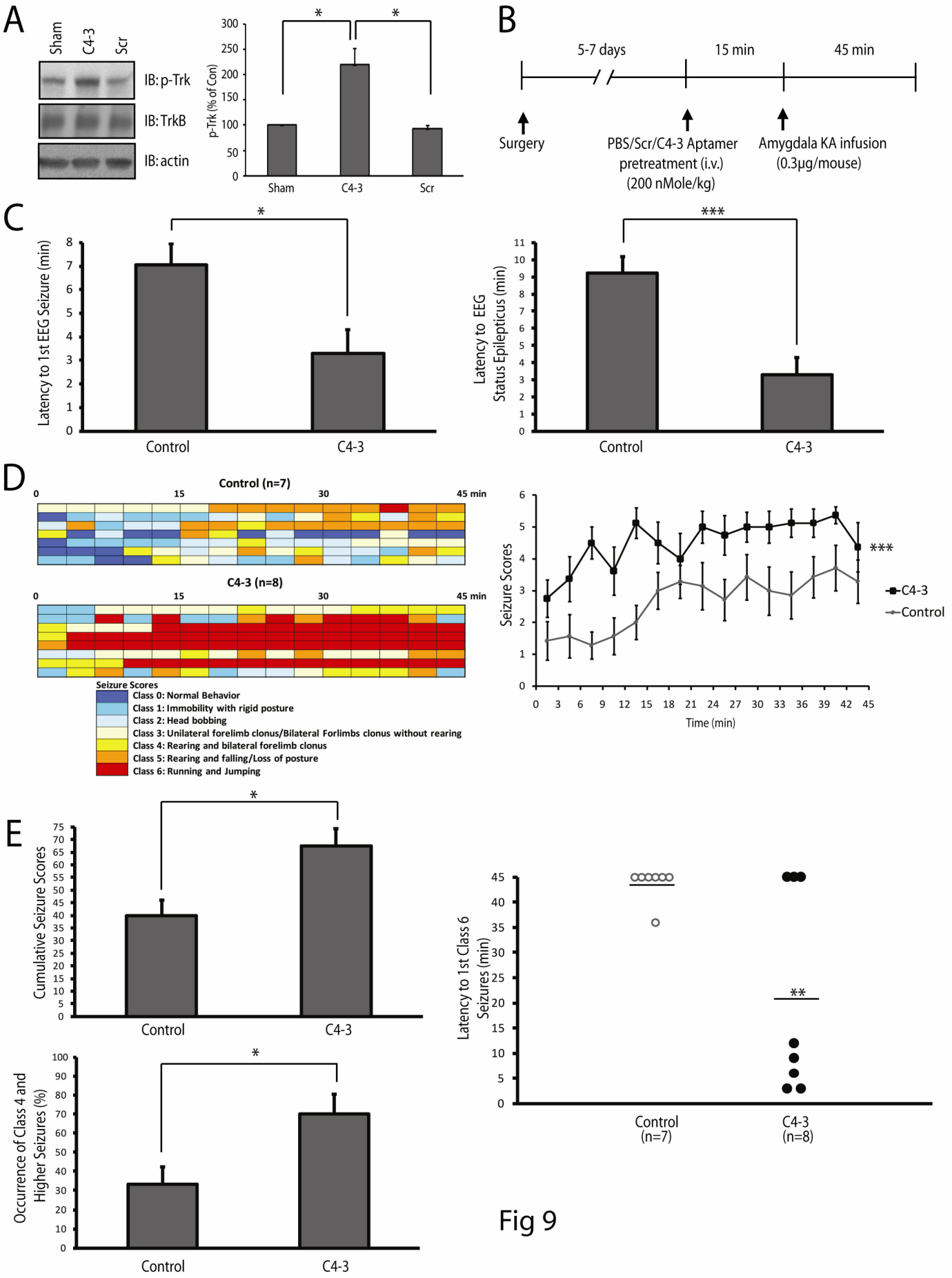
A
Sham
C4-3
Scr
IB: p-Trk
IB: TrkB
IB: actin
p-Trk (% of Con)
Sham
C4-3
Scr
B
5-7 days
15 min
45 min
Surgery
PBS/Scr/C4-3 Aptamer pretreatment (i.v.) (200 nMole/kg)
Amygdala KA infusion (0.3µg/mouse)
C
Latency to 1st EEG Seizure (min)
Control
C4-3
Latency to EEG Status Epilepticus (min)
Control
C4-3
D
Control (n=7)
C4-3 (n=8)
0
15
30
45 min
Seizure Scores
Class 0: Normal Behavior
Class 1: Immobility with rigid posture
Class 2: Head bobbing
Class 3: Unilateral forelimb clonus/Bilateral Forlimbs clonus without rearing
Class 4: Rearing and bilateral forelimb clonus
Class 5: Rearing and falling/Loss of posture
Class 6: Running and Jumping
Seizure Scores
C4-3
Control
Time (min)
E
Cumulative Seizure Scores
Control
C4-3
Occurrence of Class 4 and Higher Seizures (%)
Control
C4-3
Latency to 1st Class 6 Seizures (min)
Control (n=7)
C4-3 (n=8)

Fig 9